ABSTRACT

Title of Document: MINIMIZING REANALYSIS JUMPS DUE TO NEW OBSERVING SYSTEMS

Yan Zhou, Doctor of Philosophy, 2014

Directed By: Professor Eugenia Kalnay,
Department of Atmospheric and Oceanic Science

A major problem with reanalyses has been the presence of jumps in the climatology associated with changes in the observing system. Such changes are common in reanalysis products. These jumps became especially obvious when satellites were first introduced in 1979. After 1979, however, during the "satellite era" jumps have continued to appear whenever a new observing system was introduced. To explore possible solutions to this problem, we develop and test new methodologies to minimize these reanalysis jumps in the reanalyses time series due to new observing systems.

In the first part of this dissertation, we study a state-of-the-art reanalysis, NASA's Modern Era Retrospective-analysis for Research and Applications (MERRA thereafter). Analysis increments from the MERRA and from one reanalysis without SSM/I observations (NoSSMI thereafter) are compared and their differences are defined as correction terms. The correction terms are then introduced into the tendency equation of the forecast model, i.e., GEOS-5. The debiased reanalysis

without SSM/I observation shows improvements in almost all fields, even in the precipitation field, which is generally considered to be significantly uncertain on all time and space scales. However, the difference between the analysis increments of MERRA and NoSSMI is not just due to the assimilation of SSMI, but to the accumulated effect of the assimilation of previous SSMI observations. These produce a change in the model climatology and nonlinear interactions between the variables currently observed by SSM/I, and the variables that have been modified by previous assimilations of SSMI. The nonlinear interactions introduce an additional accumulated impact during the 2-year training period.

In the second part of this dissertation, we test a new methodology in a simpler data assimilation system, SPEEDY-LETKF, because it would be unfeasible for our computational resources to apply this method to the complex MERRA system. The new method defines the correction terms by calculating the difference of analysis increments from the following two analyses, 1) assimilating both rawinsondes (RAOB) and AIRS observations, named RaobAirs, and 2) assimilating only RAOB but with its background coming from the RaobAirs analysis at every 6-hour analysis cycle. This new method limits the growth of nonlinear interactions between variables observed by AIRS and the variables that have been modified by previous assimilation of AIRS. The results show that the new method is significantly more effective in minimizing reanalysis "jumps" compared with the method applied to MERRA system.

In the third part of this dissertation, we explore a spectral model instability problem. Imperfect SPEEDY-LETKF OSSEs are unstable when assimilating RAOB observations only. Data assimilation processes worsen this problem. We found two

methods to stabilize the imperfect SPEEDY-LETKF OSSEs. Traces of the spectral waves are also clearly present in other spectral reanalyses such as the NCEP and the ERA15, but since their resolutions are higher than that of the SPEEDY model, their impact is smaller.

MINIMIZING REANALYSIS JUMPS DUE TO NEW OBSERVING SYSTEMS

By

Yan Zhou

Dissertation submitted to the Faculty of the Graduate School of the
University of Maryland, College Park, in partial fulfillment
of the requirements for the degree of
Doctor of Philosophy
2014

Advisory Committee:
Professor Eugenia Kalnay, Chair
Professor Brian Hunt, Dean's Representative
Dr. Junye Chen
Professor James Carton
Professor Takemasa Miyoshi
Professor Kayo Ide

Table of Contents

List of Tables

List of Figures

Chapter 1: Introduction

1.1 Motivation

What is a reanalysis and why it is important? The Earth's climate is dominated by natural processes of high variability over a wide range of time and space scales, so it is impossible to describe the climate system appropriately by time averages only. Instead, continuous monitoring of climate system on a high resolution is required in order to provide reliable and longest possible datasets for the validation and development of models for the atmosphere, oceans, and land surfaces. However, research on central issues in climate research can not benefit from in situ observations alone because of their sparseness and irregular distribution. The space-based observations have better coverage but suffer from inhomogeneity spatiotemporally. For common users, raw observational data (in situ or space-based) has little utility. Significant value can be added by objectively combining observations into a numerical model using a "frozen" data assimilation method and model, which generate a grided reconstruction of the weather/climate record, or a reanalysis, not affected by climatological jumps associated with improvements in the model or data assimilation method. (Kalnay et al., 1996).

Challenges facing current reanalyses. A reanalysis consists of an observing system, a data assimilation system and an atmospheric model, ideally all kept unchaged with time. It is feasible to maintain the data assimilation and model unchanged, but in reality the observing system changes with time with the introduction of new

observing systems. Even with steady forecast model and analysis scheme, the temporal inconsistency of the observing systems is an unavoidable issue almost all reanalyses need to address. If the models were unbiased and had a perfect climatology, then the introduction of new observing systems would not introduce jumps, but with an imperfect real model, the introcuction of each new observing systems creates a jump in the climatology depicted by the reanalysis (see schematic Fig. 3.1).

The largest increase in the observing system took place in 1979, when a global observing system was established following the Global Weather Experiment with the implementation of a space-based observing system (Bengtsson, et. al, 2004). Since then, the amount of observation data to be assimilated has increased dramatically. Dee et al (2011) pointed out that reanalyses in the past few decades are especially challenging because of the rapid increase in observing systems. Satellite instruments that are introduced and/or ceased irregularly in time and their spatial coverages are expanding. Although this presents opportunities for constructing an increasingly accurate and complete description of the global climate states, it also leads to discontinuities and spurious variations in the reanalysis. These artificial discontinuities or "jumps" in reanalyses may be caused by the assimilation of biased observations, or by introducing new observations that constrain previously unobserved components of model bias.

One example is the time evolution trends of precipitation from different reanalyses (Figure 1.1). Reanalysis precipitation is generally considered to have dramatic

variability and uncertainty on all spatiotemporal scales. Figure 1.1 clearly shows the significant changes of MERRA (NASA's **M**odern **E**ra **R**etrospective-analysis for **R**esearch and **A**pplications, Rienecker et al, 2011) global mean precipitation time series in the last two decades, simultaneous with introducing or ceasing different types of satellite observations, like SSMI and ATOVS (big red arrows) This figure also illustrates that precipitation calculated from MERRA is closer to the reference (GPCP and CMAP) than other reanalyses.

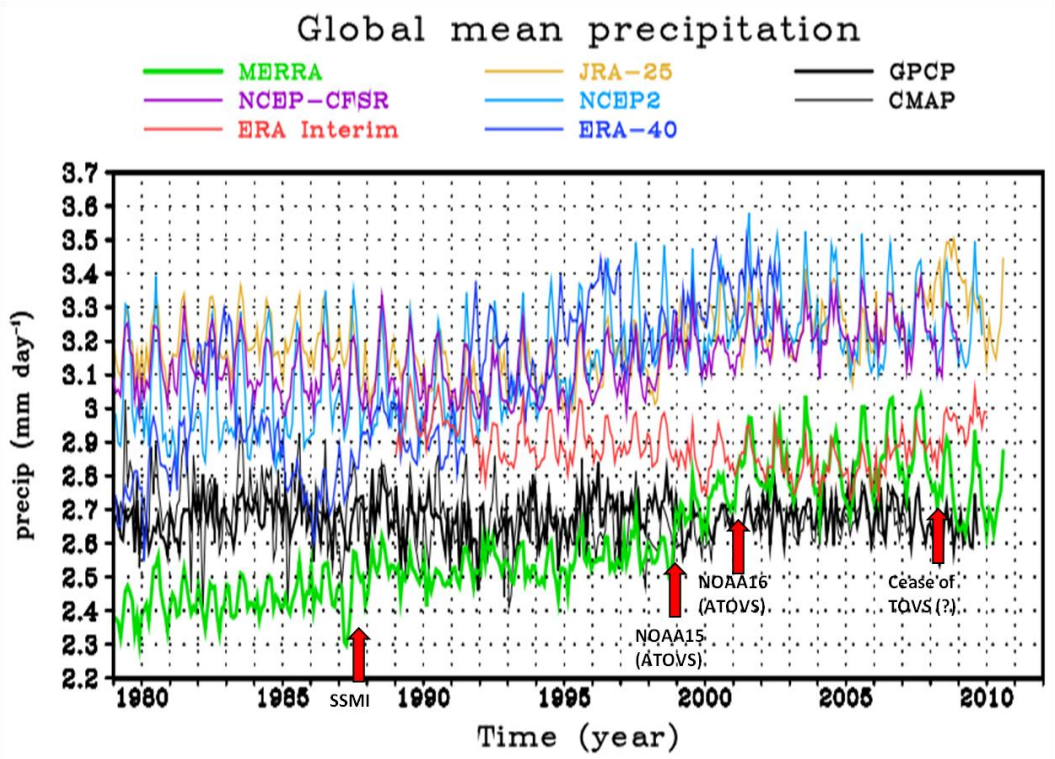

Figure 1.1 Changing observing system and its impact on MERRA (Chen et al., 2012)

1.2 Previous studies

Several previous studies had explored the impacts of changing global observing system on reanalyses. For example, Bengtsson et.al (2004) pointed out that, the

climate trends of some global qualities computed from ECMWF ERA40 reanalysis, such as temperature, integrated water vapors, and kinetic energy, were not genuine but an artifact caused by changes in the global observing system. Sterl (2004) assessed the homogeneity of ERA40 by comparing it with the NCEP–NCAR reanalysis, and also by investigating a known relationship between the modeled latent heat flux and SST. This research reminded reanalysis users not to confuse the inhomogeneity with real changes when using the reanalysis data to investigate climate change issues. Bengtsson et.al (2004) studied how to estimate the impact of selected reduced observation system on ERA40 by systematically removing observations from the present observational database to mimic the observing systems of the past.

MERRA is a state-of-the-art reanalysis, which has a complete water and energy budget that can be used to improve climate and weather models, and to characterize the hydrological system on the Earth. However, few researchers have investigated how to resolve the inhomogeneity problem in this relatively new reanalysis dataset. Robertson et al (2011) studied the effect of satellite observing system changes on MERRA water and energy fluxes. Their study reveals that principal component regression (PCR) is useful in isolating and reducing artifacts produced by changes of satellite sensors. However, The PCR technique, as well as any other linear regression methods, is not without problems, because its statistical nature prevents the ability to distinguish between trends associated with real physical processes and those arising as a consequence of the step functions. Another ongoing effort, led by Dr. Junye

Chen (2012), involves the use of multiple Reduced Observing System Segments (ROSS) experiments to determine the contribution of each observing system change to the evolving time series of MERRA reanalysis.

1.3 Objective and methodology

Objective. Our main objective is to improve the long-term homogeneity associated with the introduction of new observing systems in a reanalysis through analysis increment corrections instead of doing it *a posteriori*. In this dissertation, we develop and test new methodologies to minimize the reanalysis "jumps" in time series due to new observing systems.

Methodology. The methodology is inspired by Danforth et. al (2007). In Danforth et al (2007)'s research, a 6-hourly model forecast was compared with a reference (the NCEP-NCAR reanalysis) to generate a correction term, which was then added to the model tendency equations. The model was run again with the new tendency equations, and this much reduced the bias. In the present research, by comparing a reanalysis and its corresponding Reduced Observing System Segment (ROSS) experiment, we can obtain the bias between them due to the introduction of a new observing system. Based on this bias information, corrections could be made on the reanalysis before the introduction of the new observing system, so as to adjust the earlier period data to match with the later period data.

There are several possible methods to define the correction terms. In the present study, we generate the corrections from the differences of analysis increment fields. The corrections will be added to the tendency equation of the ROSS experiment as a new forcing term. Then, the ROSS experiment with new model tendency equation is conducted again and is expected to better reproduce the reanalysis with the new observing system.

Two data assimilation systems will be tested in this dissertation, the MERRA and a modified version of SPEEDY-LETKF system (Miyoshi 2005) provided by Dr. Ji-Sun Kang (2012). MERRA reanalysis utilizes the operational GEOS5-DAS to produce a long-term synthesis since 1979. It involves the Incremental Analysis update (IAU) procedure (Bloom et al., 1996), which eliminates the shocks that are otherwise associated with the insertion of the observations at the beginning of every analysis cycle (Schubert, 2008). The SPEEDY-LETKF is a combination of a simplified atmospheric GCM, known as SPEEDY, and the ensemble-based analysis scheme, LETKF (**L**ocal **E**nsemble **T**ransform **K**alman **F**ilter). It is a simple, computationally efficient, yet realistic Observing System Simulation Experiments (OSSE thereafter) system which has been widely used to explore difficult data assimilation problems like carbon cycle and large-scale precipitation assimilations (Kang et al. 2012, Lien et al. 2013). Details of these two analysis systems are given in Chapter 2 and Chapter 3, respectively.

1.4 A brief discussion of the reanalysis correction approaches

The first approach to correct climate "jumps" is tested in MERRA system. The differences between analysis increments from two 2-year analyses with (the MERRA reanalysis) or without assimilating SSM/I (the NoSSMI reanalysis thereafter), a satellite observing, are used as correction terms. The correction terms are then added to forecast model (GEOS-5) tendency through IAU procedure. The debiased reanalysis without SSM/I assimilation does show significant improvements in almost all fields. However, the correction is underestimated by about a factor of 2 because the analysis increments in the NoSSMI have been modified by climatological differences between the forecasts of MERRA and NoSSMI reanalyses. Such forecast differences rise because of nonlinear interactions 1) between different variables observed by SSM/I, and 2) between SSM/I and existing observing systems. The nonlinear interactions accumulate during the whole 2-year training period. So a more effective correction approach that is not affected by changes in the background climatology should be able to remove the forecast differences between MERRA and NoSSMI.

The second approach that attempts to do this is to generate corrections by comparing the following two analyses: 1) MERRA and 2) an analysis starting from MERRA forecast but withholding SSM/I assimilation at every 6-hourly analysis cycle. Since these two analyses share the same forecast, the analysis increment difference is actually the analysis difference, and the correction will not be counteracted by climatological differences between the forecasts. However, applying the second

approach in a complex operational system like MERRA is unfeasible considering our limited computational resources. Thus, this new approach will be tested in an idealized data assimilation system, the SPEEDY-LETKF. The SPEEDY-LETKF analysis assimilating both RAOB and AIRS is a counterpart of MERRA, and RAOB only is the counterpart of NoSSMI. The experiment starting from "RaobAirs" analysis but withholding AIRS observation is named "RaobAirs_noAirs".

A third approach is a simple climatological correction based on a comparison of the analyses with and without AIRS.

1.5 Outline of the dissertation

Chapter 2 describes the MERRA reanalysis system and the first approach to correct climate "jumps" based on ROSS. Chapter 3 studies the SPEEDY-LETKF system. We successfully test and compare the two analysis increment correction approaches discussed in Section 1.4 using SPEEDY-LETKF system. The climatological bias correction performed a *posteriori* (offline) is also investigated. In Chapter 4, we discuss spectral model instability problems and the efforts we made to remove the unphysical negative humidity values in out imperfect SPEEDY-LETKF OSSEs. Chapter 5 gives a summary and discusses future research directions

Chapter 2: MERRA experiments

2.1 Introduction

The primary drivers for this dissertation are to determine the contribution of each observing system change to the evolving time series of a reanalysis, and to find a solution, using data assimilation techniques, to minimize the "jumps" in the reanalysis long term climate trend due to the new observing systems. The original idea of using data assimilation technique came from Dr. Junye Chen, based on his research interest in exploring the effect of satellite observing system changes (e.g. SSM/I in late 1987, AMSU-A in late 1998) on MERRA water and energy fluxes budgets (Chen et al. 2010, Robertson et al. 2011).

Although the principal component regression (PCR) method (Robertson et al. 2011) was shown to be useful for identifying artifacts produced by changes of satellite sensors, and successfully improved the precipitation time series compared to the GPCP on a global basis, it is not without drawbacks. The PCR method, as well as any linear regression technique, could not distinguish between trends associated with physical processes and those arising as a consequence of the step functions. Since one could not expect an event like an observing sensor change to be captured by a single mode, the selection of those increment modes involved in PCR method is a subjective process. Naturally, the need for a more objective adjustment strategy is raised.

Conducting Reduced Observing System Segment (ROSS) experiments is one example of the objective, physically meaningful adjustment strategies for long-term climate trends in reanalyses. For example, Bengtsson et al. (2004) demonstrate how to estimate the global atmospheric circulation from reduced observations. Chen et al. (2010) demonstrates the impact of assimilating ATOVS radiances in MERRA by comparing a two year ROSS withholding the NOAA-15 ATOVS radiance data with the original MERRA reanalysis. Another two year ROSS withholding the SSM/I is also conducted, while the obtained information from this experiment is not discussed. However, how to use the impacts from ROSS experiments to homogenize MERRA is still a question not clearly answered.

In this chapter, we aim to use the information gathered from the ROSS experiment withholding SSM/I to minimize "jumps" in global mean precipitation time series in late 1987, through data assimilation techniques associated with the analysis increment fields. A detailed description of the MERRA system, the SSM/I satellite observation, the importance of analysis increments, etc., are given first.

2.1.1 What is MERRA?

NASA's Modern Era Retrospective-analysis for Research and Applications (MERRA, 1979-present) is a recent high-resolution reanalysis that utilizes the Earth System Modeling Framework (ESMF)-based Goddard Earth Observing System Model Version 5 (GEOS-5) as a forecast model, and the new NCEP unified grid-point statistical interpolation (GSI) analysis scheme as the data assimilation system (DAS).

With emphasis on exactly closing the water and energy budgets, MERRA surpasses other recent reanalyses in assimilating time series of global monthly mean precipitation (Rienecker et al, 2011). Many other studies have explored the hydrology features of MERRA reanalysis, e.g. Bosilovich et al. 2011, Kim et al. 2013, Lorenz et al. 2012, Reichle et al. 2011, Lindsay et al. 2014. One of the key advances of MERRA is the high resolution and frequency of the output. The analysis is performed with native spatial resolution with 1/2 degrees latitude by 2/3 degrees longitude, at 72 vertical levels that extends through the stratosphere on a terrain-following hybrid sigma-p coordinate. Two-dimensional diagnostic fields like surface fluxes are also available at native horizontal resolution at 1-hour intervals. Other products include three-dimensional, 3-hourly atmospheric diagnostic fields with 1.25 degree horizontal resolution at 42 pressure levels, etc.

The GEOS-5 AGCM includes a finite-volume dynamical core (Lin, 2004) that is found to be very effective especially for transport in the stratosphere (Pawson et al., 2007). The AGCM is coupled to a catchment-based land surface model (CLSM) (Koster et al., 2000) and a multi-layer snow model (Stieglitz et al., 2001). Its physics package, described by Bacmeister et al. (2006), includes various physical processes like moist physics parameterizations, radiation, turbulent mixing, chemical species, and surface processes. The time step of the physics parameterization is 30 minutes, though the dynamics time step is considerably shorter. The primary variables are wind components, scaled virtual potential temperature, pressure thickness, and specific humidity (Suarez et al. 2008).

The GSI (Wu et al. 2005) is a three-dimensional variational analysis system developed at NCEP (with the potential to be adapted to an ensemble Kalman filter–variational hybrid data assimilation system, e.g., Kleist 2012, Wang et al. 2013) applied in the grid-point space, which allows more flexible and straightforward applications of the background error covariances (Kleist et al, 2009). The GSI utilizes the JCSDA community radiative transfer model to assimilate radiances and rain rate directly, and a variational bias correction to the radiances is included (Schubert et al. 2008).

2.1.2 Model tendency and incremental analysis update

The MERRA reanalysis employs an incremental analysis update (IAU) procedure (Bloom et al., 1996) to minimize the spurious 6-hourly periodic perturbations in analysis caused by the observation input (Kennedy et al. 2011). The IAU variable is an analysis increment (AI) representing the difference between an analysis field and its corresponding background model state at the synoptic time, using observations during a 6-hour window centered at this synoptic time. The AI is then divided by 6-hour, or 86400s, to produce an analysis tendency, which is a forcing term in the model tendency equation (Eq(1)) (Cullather and Bosilovich 2011). The model then restarts three hours before the analysis time, and run for the same 6-hour period again, with the analysis tendency added to the normal dynamic and physics model tendencies. The new 6-hour run is referred to as the "corrector" segment of the IAU. All products from GEOS-5 are produced during the corrector segment, except for the analyses themselves. The run is then continued without an analysis tendency for the

next 6-hour window centered at the next synoptic time, and the entire cycle is then repeated. Figure 2.1 provides a schematic of the IAU implementation in GEOS-5. In this way, only the tendency of a state can have discontinuities and not the state itself. This IAU forcing term is essential for closing water and energy budgets, and for the transport of ozone and trace gases (Suarez et al. 2008).

$$\left(\frac{dZ}{dt}\right)_{total} = \left(\frac{dZ}{dt}\right)_{dyn} + \left(\frac{dZ}{dt}\right)_{phy} + \left(\frac{\boldsymbol{dZ}}{\boldsymbol{dt}}\right)_{\boldsymbol{ana}} \qquad Eq(1)$$

$$analysis\ tendency\ from\ IAU: \left(\frac{\boldsymbol{dZ}}{\boldsymbol{dt}}\right)_{\boldsymbol{ana}} = \frac{\boldsymbol{analysis\ increment}}{\boldsymbol{6hr}}$$

where $\left(\frac{dZ}{dt}\right)_{total}$ is total tendency

$\left(\frac{dZ}{dt}\right)_{dyn}$ *is GEOS5 tendency from adiabatic dynamic process*

$\left(\frac{dZ}{dt}\right)_{phy}$ *is GEOS5 tendency from diabatic physics process*

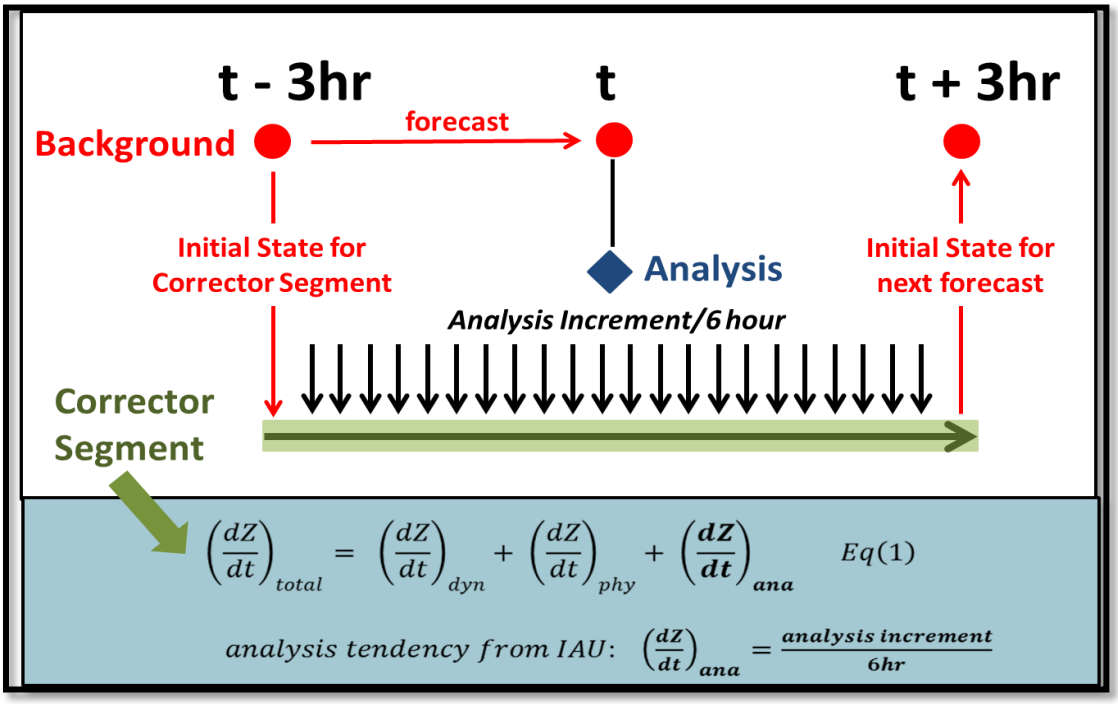

Figure 2.1 Schematic of the IAU implementation in GEOS5-DAS.

2.1.3 SSM/I observing system

Figure 1.1 indicates that there are at least four "jumps" in MERRA global mean precipitation time series. Why do we focus on the "jump" associated with the SSM/I introduced into MERRA in late 1987? One essential reason lies in the fact that only SSM/I, in conjunction with the TRMM Microwave Imager (TMI), provide the instantaneous rain rate estimates, although more than 20 observation data sources are assimilated (Table 3.5.1 of Suarez et al. 2008). The forward model of the instantaneous rain rate estimates need synoptic inputs like surface pressure, temperature, winds, etc. However, it is most sensitive to the moisture and cloud condensate. The second reason why we are focusing on SSM/I is based on the finding that, introducing SSM/I into MERRA in late 1987 apparently tends to "decrease the drying from other observations in the subtropics but dries the high latitudes, particularly in the SH." (Robertson et.al. 2011). We need further studies of the impacts of assimilating the SSM/I observation, and find a solution how to minimize the discontinuity in the MERRA caused by introducing it.

The SSM/I instrument on satellites uses a unified, physically based algorithm to simultaneously retrieve ocean wind speed (at 10 meters), atmospheric water vapor, cloud liquid water, and rain rate. The SSM/I channels are sensitive to water vapor, cloud, precipitation and surface parameters, rather than temperature. SSM/I radiances are only assimilated over clear-sky ocean; observations over land or ice are excluded. For more technical details of SSM/I, please refer to the website of Remote Sensing

Systems, a private research company processes microwave data collected by special satellite microwave sensors (http://www.remss.com/missions/ssmi).

2.2 Hypothesis

By comparing MERRA data and a ROSS without SSM/I observation assimilation, named NoSSMI thereafter, we can obtain the bias between MERRA and NoSSMI due to the introduction of a new observing system. Based on this bias information, corrections can be made on the MERRA reanalysis before the introduction of the new observing system, so as to adjust the climatology of the earlier period data to match with the later period data. There are several possible methods to obtain the bias and to make the correction. In this study, we aim to make the correction in the IAU process (Fig. 1.2). The correction terms will be derived from the bias of analysis increments between the original MERRA data and the NoSSMI.

2.3 Experiment design

As indicated in Chapter 1, the methodology we propose here is inspired by Danforth et al (2007, DKM2007 hereafter) who compare model data with a reference (the NCEP-NCAR Reanalysis) to generate analysis corrections. The model is then run again adding the analysis correction as a forcing term in the model tendency equation, named a debiased model. In this way, the correction is made during the model integration instead of a posteriori statistical correction as done in short term climate

predictions (vanden Dool, 2005). The debiased model exhibits significantly lower bias in 6-hour as well as extended forecasts (DKM2007).

In present study, if MERRA was considered as reference, NoSSMI would represent the biased reanalysis. The correction is defined as the bias of analysis increments between MERRA and NoSSMI, for any combination of moisture, temperature, and wind fields, as shown in schematic Figure 2.2. Since SSM/I was assimilated by MERRA since July 1987, the 2-year training period is July 1987 to June 1989. The 2-year long, 6-hourly dataset is then averaged at the same time of a year, producing a 1-year long, 6-hourly dataset. We will show in Section 2.4 that the analysis increments of both MERRA and NoSSMI have very clear and similar annual cycles. So averaging at the same time of a year gives a smoother, representative analysis increment field. The correction can be applied to the MERRA before SSM/I was introduced, and expected to minimize the discontinuity associated with it (dashed green line before July 1st 1987). Note that the troposphere processes of the MERRA will adjust to new observation in about 2 weeks (Chen, pers. comm., 2012). How to deal with the adjusting period (grey shaded area) is still unknown and worth further study.

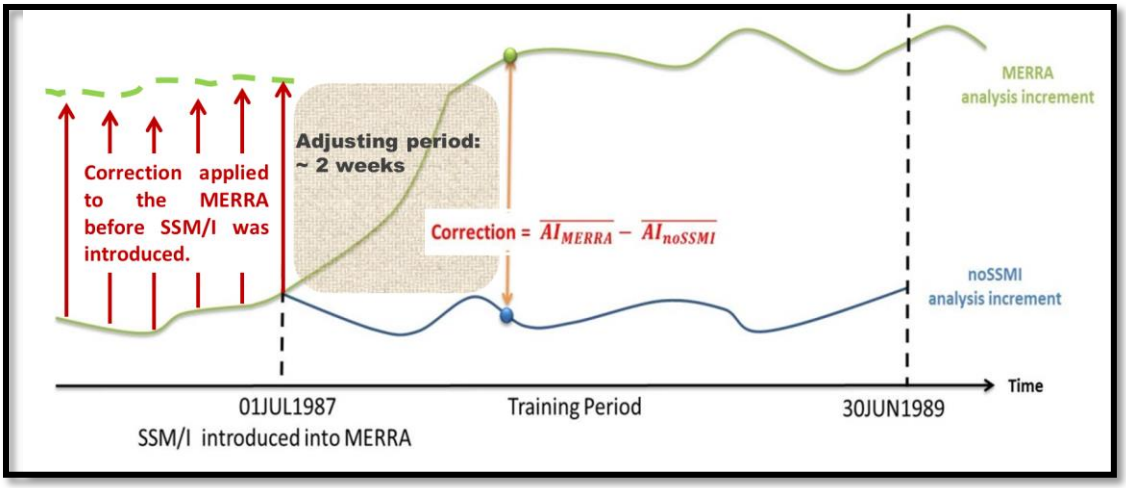

Figure 2.2. Schematic on correction definition.
Correction = analysis increment bias = $AI_{MERRA} - AI_{noSSMI}$

The 365-day correction, after Fourier transform, will be imported to IAU produced analysis increment every six hour, at the corresponding time within a year, to test whether this correction can force NoSSMI to approach MERRA in a climatological sense). If successful, we can apply this correction in the period before SSM/I was introduced to minimize the discontinuity in MERRA. The purpose of conducting Fourier transform of the annual cycle of the differences is to reduce sampling error in the correction data. We do not conduct spatial Fourier fileting because of major goal is to improve the global reanalysis homogeneity in time. How to remove the spatial noise in the correction terms are left for further research.

The question now is on which field(s) should we correct? Considering the complex interrelationship with the variables of SSM/I, we need to think carefully before adding the correction to the NoSSMI reanalysis. Figure 2.3 (by courtesy of Chen. et

al, 2012) shows the zonal mean differences in summer (JJA) between MERRA and the NoSSMI runs, and explains how moisture impacts temperature state in SSM/I data. The specific humidity (Q) increment and humidity itself have positive signs, meaning that the effect of SSM/I is to add water vapor into the system (a positive Q increment) and enhance the Q field to higher value (positive Q). The extra water vapor from SSM/I leads to more precipitation and more latent heat release, so there are positive changes in temperature field (T). This positive T field change induces a negative T increment from other observations, in order to balance the extra latent heat release from precipitation. This cause and effect chain explains the same sign observed between MERRA and NoSSMI humidity fields and analysis increments but opposite signs for T and its analysis increments as shown in Figure 2.3. It also proves that humidity is the "driver" variable in SSM/I observation. Thus, we begin experiments with specific humidity correction, followed by specific humidity and temperature correction, and finally a correction in humidity, temperature, and wind fields all together. Table 2.1 gives experiment scenarios.

Experiment name	the correction(s) applied
add_Q	Specific humidity
add_Q&T	Specific humidity and temperature
add_U&V&T&Q	Specific humidity, temperature, U, and V
add_2Q	2*Specific humidity

Table 2.1 Correction on NoSSMI experiment scenarios

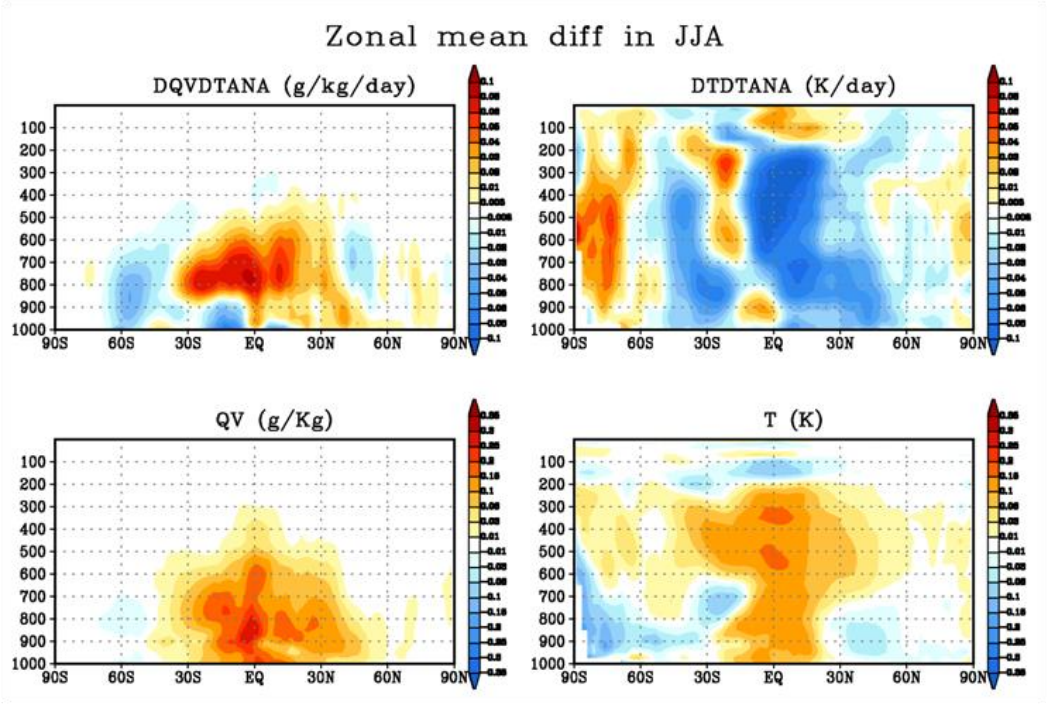

Figure 2.3. Specific humidity and temperature zonal mean difference between MERRA and NoSSMI experiments (by courtesy of Chen et al, 2012). Upper left: humidity analysis increment. Lower left: humidity difference. Upper right: temperature analysis increment. Lower right: temperature difference.

2.4 Results and challenges

We want to point out that the results from add_Q&T and add_U&V&T&Q experiments have no significant differences from those obtained with the experiment add_Q, so they are not shown is this section. This is reasonable because humidity is the "driver" variables in SSM/I observation, and the other variables are modified by the addition of Q. The correction in humidity field (add_Q) is only partially successful because it is too weak. Then, we double the humidity correction terms in the model tendency equation, and do the add_2Q experiment, to explore if astronger correction terms can make the debiased analysis climatology resemble MERRA better.

2.4.1 Estimation of the specific humidity climatological analysis increment

Figure 2.4 shows the monthly analysis increments of specific humidity from the MERRA (black) and the NoSSMI (green) reanalyses, during July 1987 to June 1989. The three columns represent different regions, the NH mid-latitude (left), the Tropics (middle), and the SH mid-latitude (right). The three rows represent 200hPa, 500hPa, and 925hPa respectively from top to bottom. The analysis increments from both reanalyses show clear annual and seasonal cycles, especially over the NH mid-latitude area. This is because the climate of the northern hemisphere mid-latitude is more stable and the observation is more abundant in this region. Figure 2.4 also demonstrates that analysis increment of specific humidity) differences are larger in the Tropics and at lower levels.

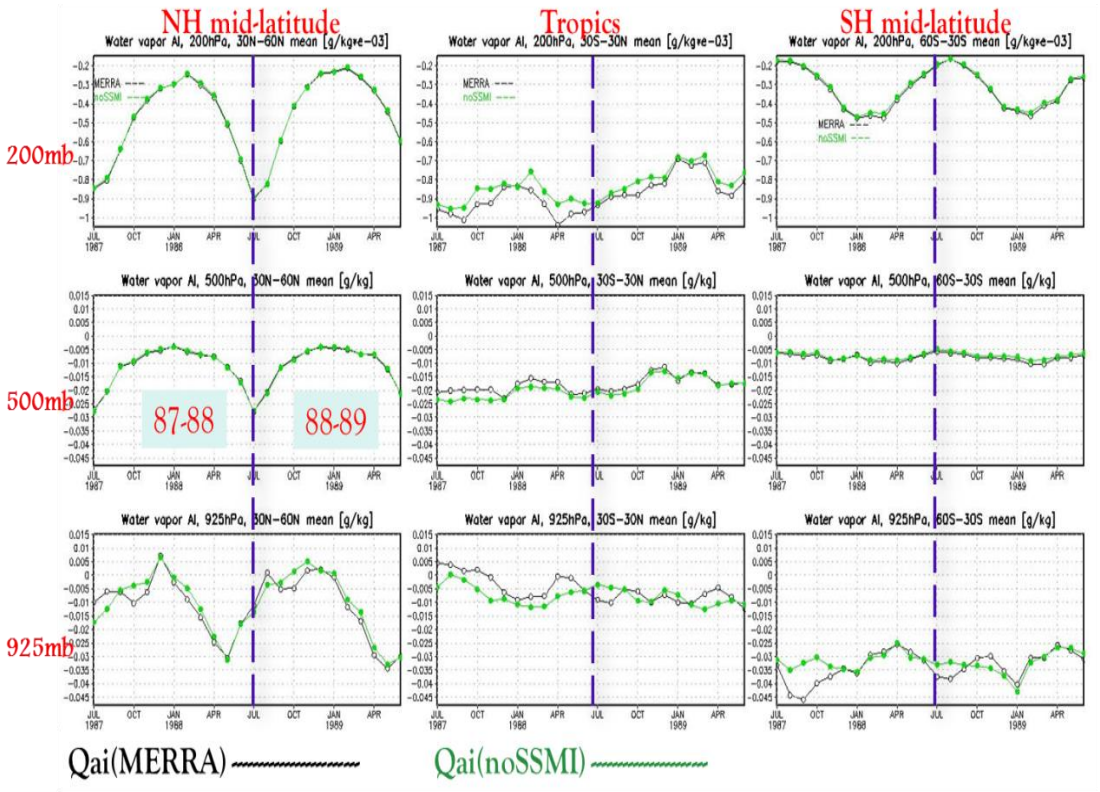

Figure 2.4. Monthly specific humidity analysis increment time series

In order to remove sampling errors from daily observation, before introducing into the GEOS-5 model tendency, we apply a Fourier transform to the annual correction, i.e. to the specific humidity analysis increment bias between MERRA and NoSSMI experiments, and retain only the first three terms. Figure 2.5 shows the specific humidity correction in July and its corresponding Fourier filtered fields that combine annual mean, semi-annual, and seasonal oscillations. It clearly illustrates that the limited Fourier series truncation that we use to reduce sampling errors is sufficient to represent fairly well the climatology of the observed humidity analysis increment difference between MERRA and NoSSMI experiments and reduce the sampling errors. This is also true for other variables of the analysis, like T, U, and V (not shown).

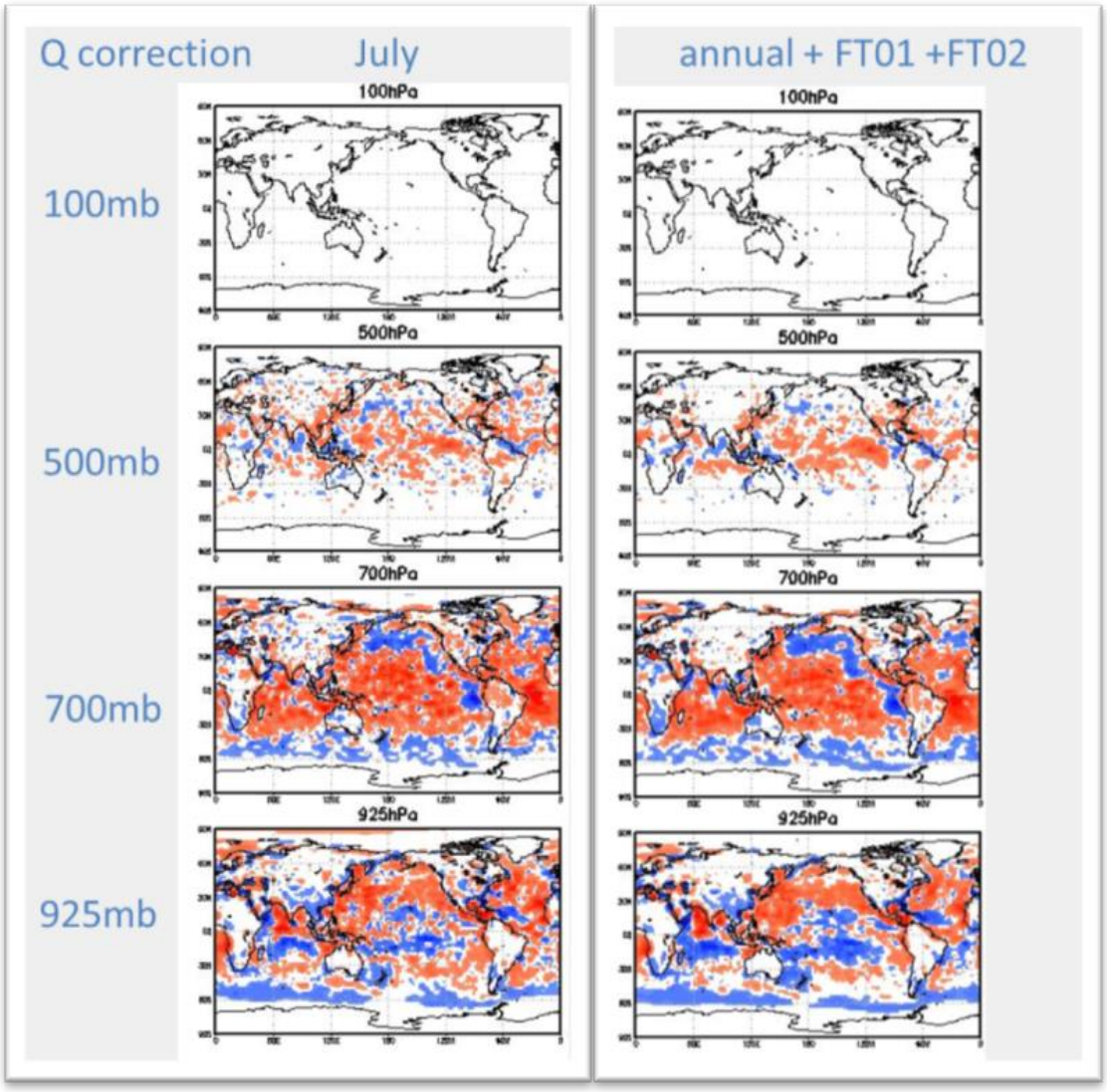

Figure 2.5 Specific humidity (Q) correction and its Fourier transfer. 1st column: Q correction July mean; 2nd column: Q correction combining annual mean, semi-annual oscillation (FT01), and seasonal oscillation (FT02).

2.4.2 Total precipitable water and precipitation from debiased experiments

In the following figures we compare the results obtained in MERRA with those obtained with NoSSMI, and add_Q, and add_2Q. If our approach was working well we would expect that add_Q would become climatologically similar to MERRA. We

will see that the corrections in add_Q have the right sign, but are too weak, so that add_2Q is actually closer to MERRA.

Daily total precipitable water (TQV) global mean is shown in Figure 2.6, for July – November, 1987. MERRA (red) contains more moisture than NoSSMI experiment (green). The debiased experiment add_Q (orange) follows the trend of NoSSMI and shows improvements in TQV global mean filed. However, this improvement is not strong enough. Actually, doubling the humidity correction term leads to greater improvement. The global mean TQV time trend from add_2Q experiment (black) agrees with that from MERRA quite well.

Figure 2.7 shows the daily total precipitable water bias, comparing MERRA, add_Q, and add_2Q experiments with NoSSMI experiment. Allowing for the spin-up and seasonal change issues, we make the total precipitable water (TQV) spatial comparison maps based on September to November data only. The spatial distribution from add_Q experiment (middle panel) is closer to MERRA than the NoSSMI(top panel). It is able to catch the cold bias in the Indian Ocean, but fails to simulate the warm bias in the central to eastern equatorial Pacific Ocean, and the equatorial Atlantic Ocean. However, add_2Q experiment (bottom panel) presents closer results to MERRA, in both spatial pattern and magnitude.

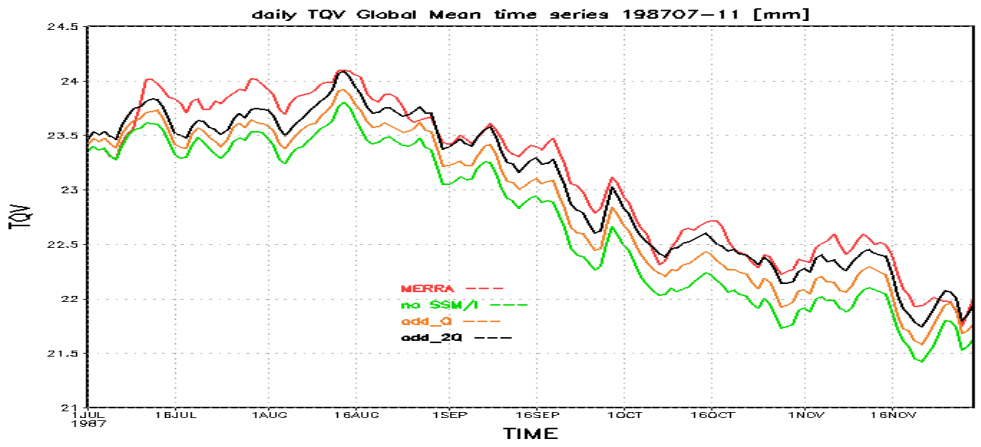

Figure 2.6. Daily total precipitable water (TQV) global mean, July – Nov 1987 time series

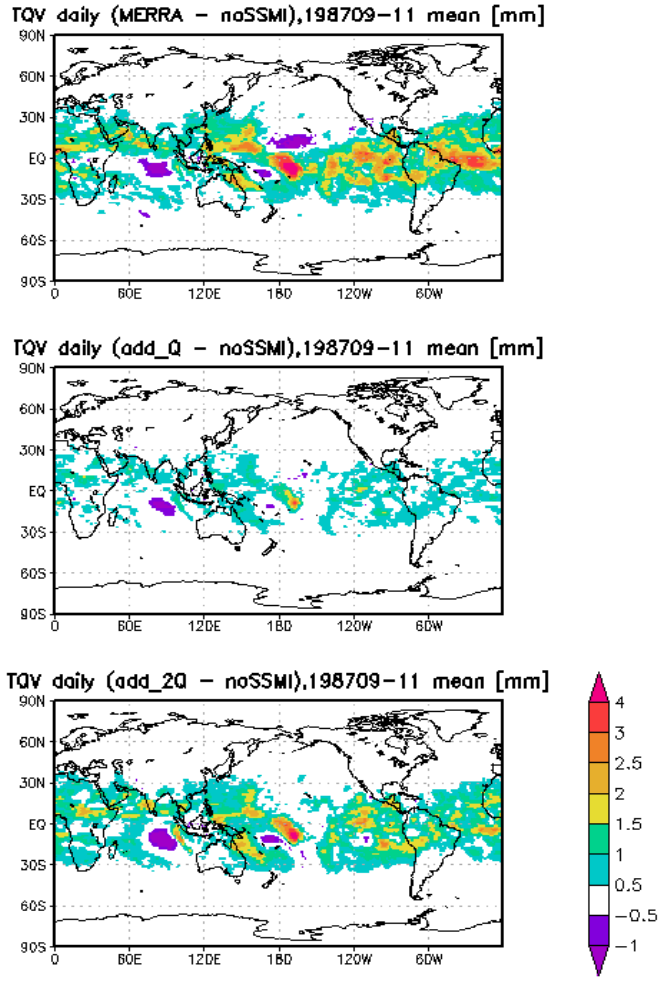

Figure 2.7 1987 September to November average of daily total precipitable water (TQV) bias. From top to bottom, the panels are biases between MERRA and NoSSMI, add_Q and NoSSMI, and add_2Q and NoSSMI.

Similar results can be found in the precipitation field. The global average of daily-accumulated precipitation is shown in Figure 2.8, from July-November 1987. As discussed above, the forward model of the instantaneous rain rate estimates is most sensitive to the moisture and cloud condensate. With more moisture assimilated, MERRA (red) produces stronger precipitation than NoSSMI analysis (green). Adding the correction Q (orange) is not enough to compensate for this bias between MERRA and NoSSMI. Add_2Q (black) analysis produces more precipitation than add_Q. and is closer to MERRA than NoSSMI.

September to November average of daily precipitation bias is given in Figure 2.9. The add_Q experiment (middle panel) does not catch the strong positive precipitation bias in equatorial region as show in the top panel. The precipitation data generated by add_2Q experiment (bottom panel) agrees with MERRA precipitation in the equatorial region, but fails to resemble the negative bias around 60°S.

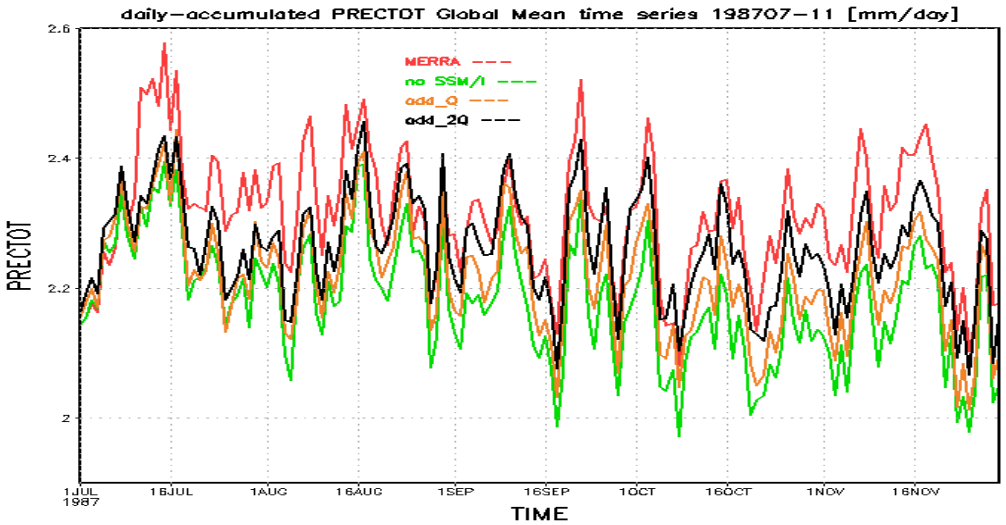

Figure 2.8. Daily-accumulated precipitation global mean, July – Nov 1987 time series

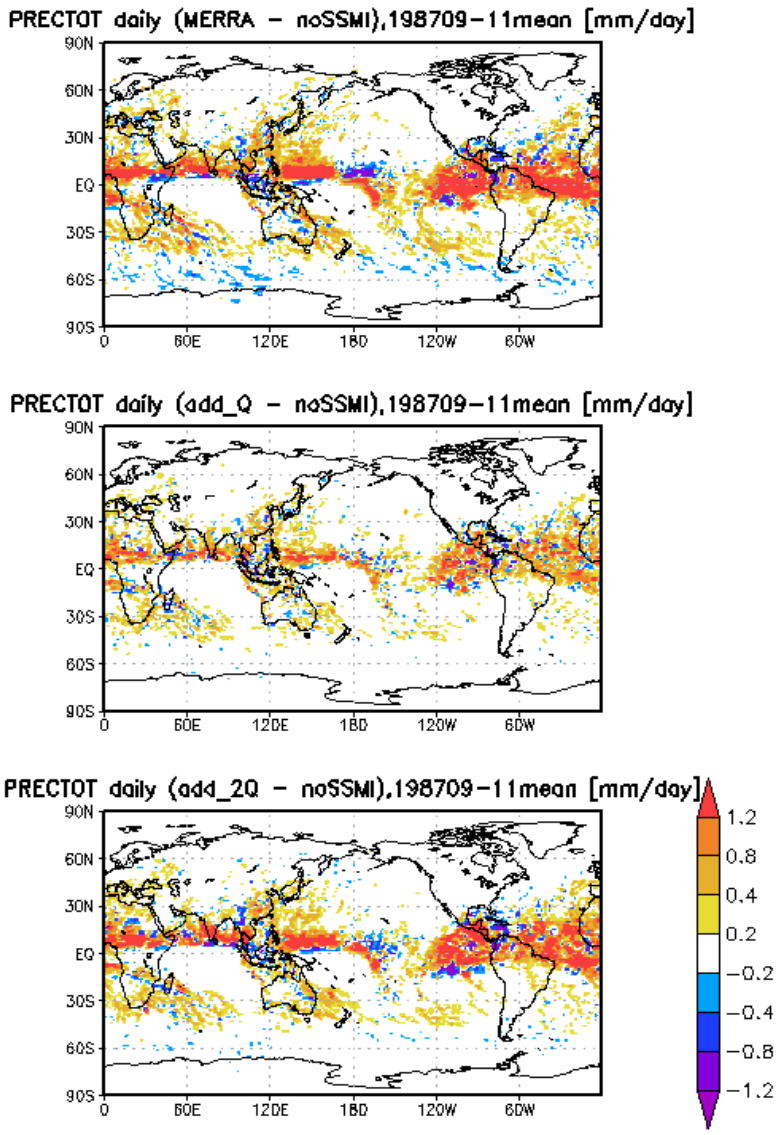

Figure 2.9. Same as Figure 2.7 but for daily-accumulated precipitation

2.4.3 Improvements for other variables from debiased models

Even though the correction was only applied in specific humidity, all major model states (Q, T, U, and V) got improved. This may be explained like this: the humidity correction in the GEOS-5 tendency introduces more moisture (Figure 2.10) into the model, and thus more precipitation and latent heat released to the air. Then, the air temperature rises (Figure 2.11). The add_2Q experiment doubles the humidity correction, which means more moisture. Thus, more precipitation and higher temperature are observed. The new thermodynamic state also impacts the dynamic fields like U and V through the thermal wind relationship (not shown).

Figures 2.10 presents the September to November average of specific humidity bias at 100hPa, 500hPa, and 925hPa levels (from top to bottom panels). The columns represent bias between NoSSMI and MERRA (left), add_Q (middle), and add_2Q (right) respectively. Figure 2.11 is similar to Figure 2.10 but for temperature field. We find that add_2Q exceeds add_Q experiment for both variables at every level and is closer to MERRA-NoSSMI, again indicating that the bias correction obtained by subtracting the NoSSMI analysis increments is of the right sign but too weak, underestimated by a factor of at least 2.

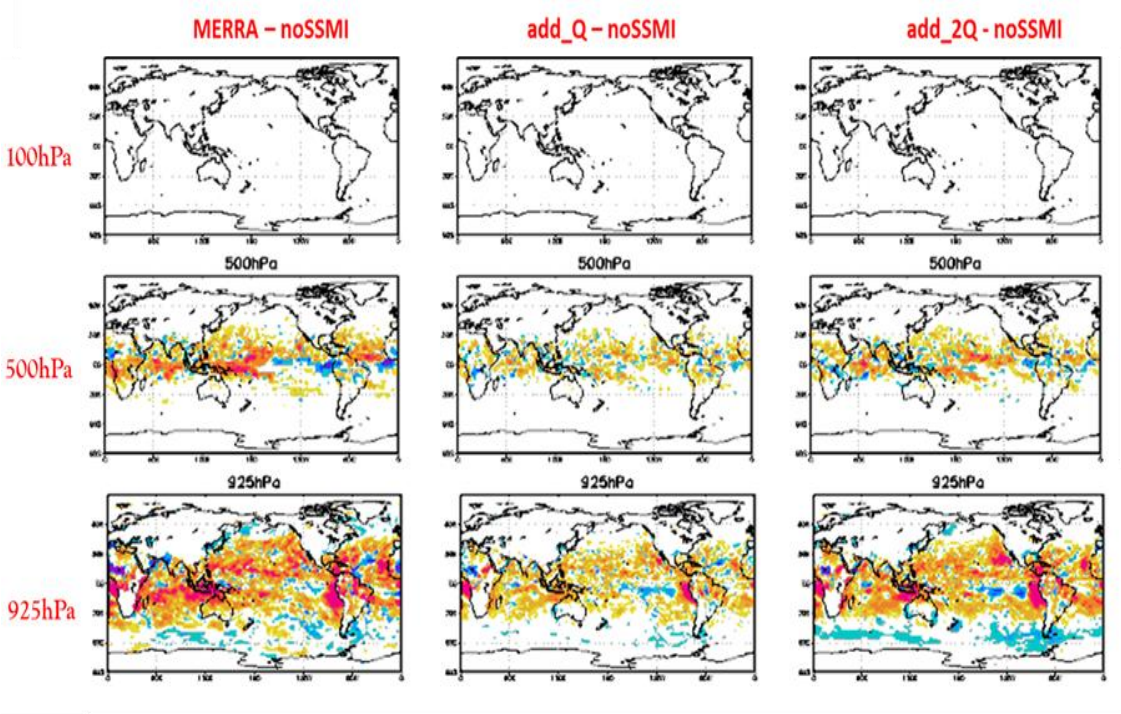

Figure 2.10. Septempber to November average of specific humidity bias. From top to bottom are 100mb, 500mb, and 925mb. From left to right columns are bias between MERRA and NoSSMI, add_Q and NoSSMI, and add_2Q and NoSSMI respectively.

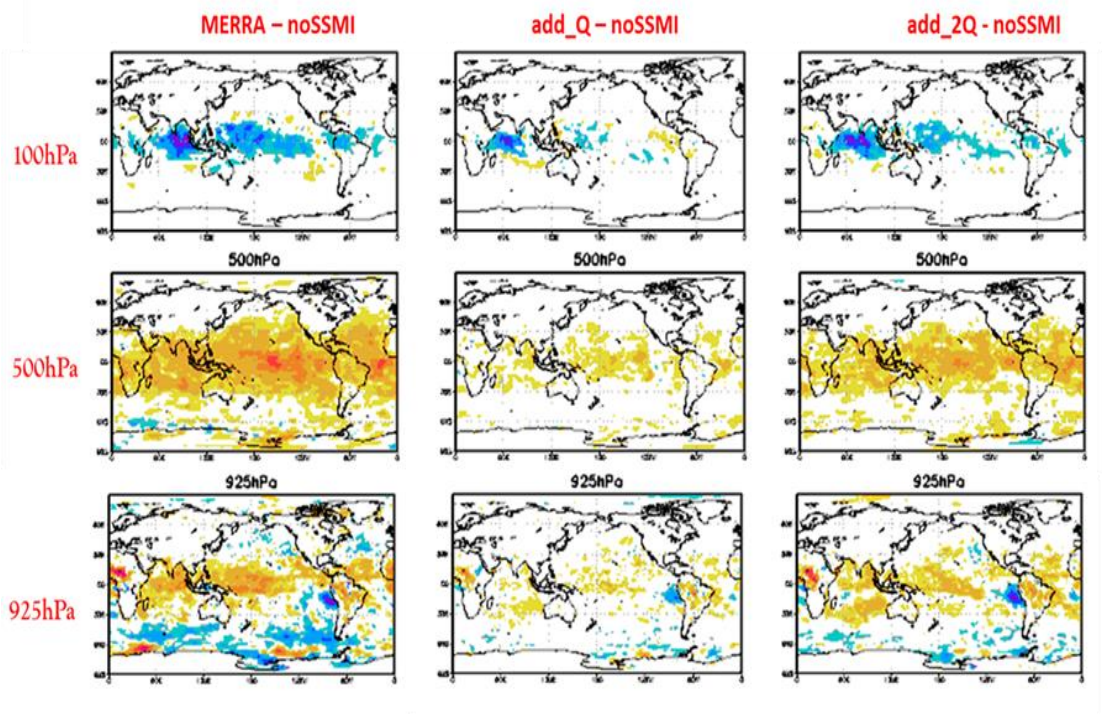

Figure 2.11. Same as Figure 2.10 but for temperature

2.5 Conclusions for Chapter 2

In Chapter 2, we investigate the impact of assimilating SSM/I observing system in MERRA since July 1987, and apply an online correction method which aims to minimize the discontinuity in humidity and precipitation fields associated with this new observing system introduction. The online correction method is to add a correction term in humidity field to the GEOS-5 AGCM model tendency equation through IAU process. We focus on moisture correction because it is the "driver" of all variables in SSM/I observation. The correction term is obtained by taking the difference between the analysis increments of MERRA and NoSSMI experiments during July 1987 until June 1989.

The main result we have obtained is that correcting the NoSSMI reanalysis with the humidity analysis increment difference between the MERRA and NoSSMI experiments is only partially successful because it is too weak. In fact, doubling the humidity correction gives results that are much closer to the original MERRA. Although the correction is only applied to humidity, other variables, both prognostic and diagnostic, like precipitation, temperature and winds, all show similar improvements. Since the Q correction works but is not as good as we expected, it is possible to multiply the Q correction by a parameter and find a best value to make the debiased reanalysis resemble the MERRA. However, the new approach presented in the next chapter (DKM2007) should be optimal.

We pose two hypotheses explaining why our goal of smoothing climate "jumps" using humidity analysis increment as correction term is not achieved. The first possible reason is that the analysis increment is much smaller in amplitude than other dominant terms in the vertically integrated water vapor budget, such as the atmospheric transport, precipitation, and evaporation. However, it is still much larger than the storage term (the total change in integrated water vapor) that its contribution cannot be ignored in the overall budget (Rienecker et al. 2011). This explains why correcting humidity analysis tendency drags NoSSMI water vapor budget towards MERRA but the improvement is not as remarkable as we expected.

The second and more viable hypothesis is that the difference between the analysis increments of MERRA and NoSSMI is not just due to the assimilation of SSMI, but to the accumulated effect of the assimilation of previous SSMI observations. These produce a change in the model climatology and nonlinear interactions between the variables currently observed by SSM/I, and the variables that have been modified by previous assimilations of SSMI. The nonlinear interactions would introduce accumulated impacts during the 2-year experiment period. Therefore, the proper correction should be made by comparing the analysis increments from MERRA and from an analysis also starting from MERRA at every 6-hour cycle but withholding SSMI observation in analysis process (Figure 2.12). The correction obtained using

this new method is assumed to be linear within each 6-hour analysis cycle and does not contain accumulated nonlinear errors discussed above.

Unfortunately, it is unfeasible to explore this new method in the complex MERRA system using our current meager computational resources. Thus, the proposed new method will be applied to a simpler, ideal data assimilation system, SPEEDY-LETKF which will be discussed in the next chapter.

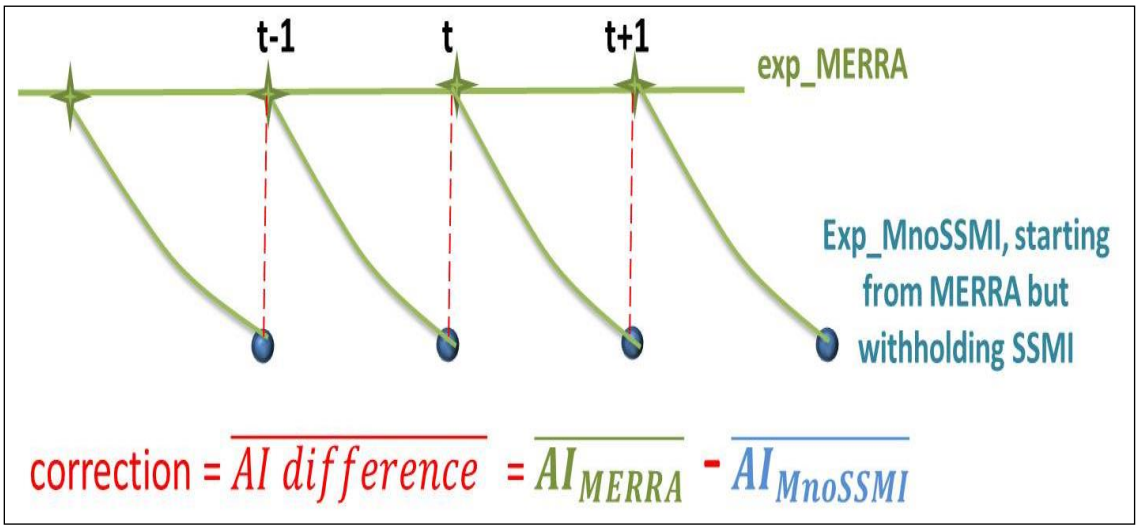

Figure 2.12 Schematic on 6-hourly correction definition in MERRA system

Chapter 3: SPEEDY-LETKF experiment

3.1 Introduction

In the previous chapter, we explored a reanalysis homogenization strategy using the MERRA system. This strategy calculates the correction terms by comparing analysis increments of two 2-year runs, i.e., the MERRA and NoSSMI, and is only partially successful, introducing corrections of the right sign to all variables, but too weak. This is referred to as **MERRA method**. Then, we proposed a more complicated method to generate correction terms, as in schematic Fig. 2.11. We first need to create an analysis *whose forecasts start from the MERRA reanalysis 6 hours before current analysis time*, but withholding SSM/I observation in analysis process. Unlike NoSSMI whose model errors accumulate over the experiment and become different from the MERRA, this new series of analyses will have the same model error of the MERRA since they share the same integration model and initial condition. Because of the fixed model error and data assimilation strategy, the impact of changing observing systems can be isolated. The analysis increment difference between the MERRA and this new series analysis is then used to calculate the correction term. This new method is inspired by Danforth et al. (2007), denoted as **DKM2007 method**. However, our limited computational resources prevent us from applying this new method using the complex MERRA system.

In this chapter, we will test both of the MERRA method and the DKM2007 method in a simpler, computationally inexpensive, but still realistic data assimilation system, a modified version of SPEEDY-LETKF system (Miyoshi 2005) provided by Dr. Ji-Sun Kang (2012). Using a simpler data assimilation system can avoid many uncertain problems that we cannot explain in a complex system, and allow easy implementation with low computational expense. We create observations from two simulated observing systems, conventional rawinsondes (RAOB), and retrievals from the Atmospheric Infrared Sounder (AIRS). A simple climatological bias correction performed *a posteriori* will also be investigated, in order to compare with the MERRA method and the DKM2007 method using analysis increment differences to correct forecast model tendencies.

3.1.1 SPEEDY-LETKF system

What is the SPEEDY-LETKF system? SPEEDY-LETKF is an analysis system, with SPEEDY as its forecast model, and LETKF as its data assimilation strategy. Its code can be downloaded at the public Google Code platform created and maintained by Prof. Takemasa Miyoshi (http://code.google.com/p/miyoshi/).

SPEEDY stands for Simplified Parameterizations, primitivE-Equation Dynamics. We are using Version 32 for the analysis system. It is a hydrostatic, σ-coordinate, spectral

Atmospheric General Circulation Model (AGCM) of intermediate complexity, developed by Molteni (2003). The version used in present study has a horizontal resolution corresponding to a triangular spectral truncation at total wavenumber 30 (T30), with a Gaussian grid of 96 by 48 points (about 400km horizontal resolution). There are 7 vertical levels at σ values of 0.08, 0.20, 0.34, 0.51, 0.685, 0.835 and 0.95. The prognostic variables include vorticity, divergence, temperature, and the logarithm of surface pressure (i.e. Vor, Div, T, and log(Ps)). Specific humidity (Q) is calculated by advection, with sinks (condensation) and sources (evaporation) determined by the physical parameterizations.

LETKF stands for Local Ensemble Transform Kalman Filter (Hunt et al. 2007). It is an efficient method to implement EnKF because the analysis and background error covariance computation is performed in low dimensional ensemble space. LETKF can naturally be computed in parallel because the analysis is done in a local domain around each grid point. The formulation of LETKF (Equations (3.1) to (3.7)) presented here follows Equations (1.1) to (1.7) of Kang (2009).

$$\mathbf{y}^{b(i)} = \mathbf{H}\mathbf{x}^{b(i)} \ , \ i = 1,2,...k \quad (3.1)$$

where k is the ensemble size (**20** in present study), $\mathbf{x}^{b(i)}$ is the i-th member of ensemble forecast, **H** is the global observation operator which interpolates forecast to observation locations, and $\mathbf{y}^{b(i)}$ is the i-th member of ensemble forecast observation.

$$\mathbf{Y}^b = \left[\mathbf{y}^{b(i)} - \bar{\mathbf{y}}^b\right] \quad (3.2)$$

$$\mathbf{X}^b = \left[\mathbf{x}^{b(i)} - \bar{\mathbf{x}}^b\right] \quad (3.3)$$

The deviations of ensemble forecast observation and ensemble forecast from their respective ensemble means are given by Equation (3.2) and (3.3). Equations (3.1) to (3.3) are computed globally before doing local computations. Then, the analysis mean ($\bar{x}^a$), the deviation of ensemble analysis ($\mathbf{X}^a$), and the analysis error covariance ($\mathbf{P}^a$) are computed in each local domain centered around each grid point.

$$\bar{x}^a = \bar{x}^b + \mathbf{X}^b \mathbf{K} (y^o - \bar{y}^b) \quad (3.4)$$

$$\mathbf{K} = [(\mathbf{Y}^b)^T \mathbf{R}^{-1} \mathbf{Y}^b + (k-1)\mathbf{I}]^{-1} (\mathbf{Y}^b)^T \mathbf{R}^{-1} \quad (3.5)$$

$$\mathbf{X}^a = \mathbf{X}^b [(k-1)\, \mathbf{P}^a]^{1/2} \quad (3.6)$$

$$\mathbf{P}^a = [(\mathbf{Y}^b)^T \mathbf{R}^{-1} \mathbf{Y}^b + (k-1)\mathbf{I}]^{-1} \quad (3.7)$$

Here y^o is vector of observations, **K** is the Kalman gain matrix, and **R** is the given observation error covariance.

Since SPEEDY is a spectral model, it has a strong tendency to create negative specific humidity values at the highest 3 levels, especially during data assimilation. Thus at the top 3 levels, the specific humidity (Q) observation is not assimilated (Miyoshi, pers. comm., 2012) and the Q analysis is not updated by any observations (i.e., in the top 3 levels, the Q analysis is equal to its background).

The localization in space is introduced because the background error covariance estimated by ensemble perturbations is a good representation of real correlation for

short distance up to 500-1000km, beyond which it becomes dominated by noise. Hunt et al. (2007) proposed an R-localization by multiplying the observation error covariance by the inversion of a Gaussian function (Greybush et al. 2011). The horizontal localization length scale used in this research is 500km.

The adaptive multiplicative inflation technique used in the current SPEEDY-LETKF system was introduced by Miyoshi (2011). It is called "adaptive" because the inflation factor is flow dependent and strongly influenced by observation density. The estimated adaptive multiplicative inflation factor tends to be large (small) over observation rich (poor) regions, so it overcomes the common problem of background uncertainty underestimation in most ensemble-based data assimilation schemes.

3.1.2 RAOB and AIRS observing systems

The SPEEDY-LETKF system provided by Dr. Ji-Sun Kang is different from the version of Miyoshi's in several ways. The major difference comes from their observing systems. The online version simply assimilates the conventional RAOB every 6 hours, while Dr. Kang's system assimilates meteorological RAOB observation, U, V, T, and Q every 12 hours (00Z and 12Z), evenly distributed Ps observation (every 3×3 grid point globally) every 6 hours, and AIRS temperature and specific humidity retrievals every 6 hours. The Figure 1 in Kang et al. (2012) provides a detailed observing system spatial distribution. The analysis assimilating both RAOB and AIRS is named as "RaobAirs", and "Raob" if assimilating RAOB

only. An analysis using RaobAirs's background but withholding AIRS observation is also conducted, named "RaobAirs_noAirs". If we conducted an imperfect observing system simulation experiment (OSSE) assimilating RAOB alone, the only type of observation available at 06Z and 18Z would be surface pressure (Ps). It is an important source contributing to the model instability (Kayo Ide and Catherine Thomas, pers. comm. 2012). The imperfect OSSE observing only RAOB blows up after about 2-month of analysis. We will come back to this issue in section 3.3.1 and 3.3.2. A summary of RAOB and AIRS observing systems is given in Table 3.1.

Observing system	Variables	Assimilation window	# of observation assimilated
RAOB	U, V, T, Q	12 hours (00Z and 12Z)	~17000 (00Z and 12Z)
evenly distributed 3×3 grid point	Ps	6 hours	~7600 (06Z and 18Z)
AIRS	T, Q	6 hours	

Table 3.1 A summary of ROAB and AIRS observing systems.

Table 3.1 indicates that there are large oscillations in assimilated observation numbers between 00, 12Z and 06, 18Z (17000 *vs*. 7600). However, we assume that the observation network evolve in time very slow when estimating the adaptive multiplicative inflation. So the estimated inflation factor at a certain analysis time would not be suitable to apply 6 hours after. In order to solve this problem, Kang et al. (2012) create a "leap-frog" cycle of adaptive inflation to update the inflation factors only when the observation network is similar. Because the RAOB meteorological

observation updates every 12 hours, the inflation interval is chosen to be $2\Delta t$ = 12 hour (Δt = 6hour, is the analysis cycle interval).

3.1.3 A Comparison of the MERRA and SPEEDY-LETKF systems

Before conducting any SPEEDY-LETKF experiment, it is worth comparing the MERRA and the SPEEDY-LETKF system so we can analyze why the same correcting method gives different results in this two data assimilation systems.

- Resolutions: the MERRA's native spatial resolution is 1/2 degrees latitude by 2/3 degrees longitude, with 72 vertical levels on a terrain-following hybrid sigma-p coordinate. SPEEDY-LETKF's is a spectral model, with a Gaussian grid of 96 by 48 horizontal grid points (about $3.75^{o} \times 3.75^{o}$), and 7 vertical sigma levels.
- Land surface descriptions: GEOS-5 is coupled to the CLSM to model the land surface, and its surface below each atmospheric column consists of a set of tiles that represent four surface types: Ocean, Land, Ice, and Lake (Suarez 2008, Appendix G). On the other hand, SPEEDY has a land-sea mask, and uses climatological variables, like SST, soil moisture, surface albedo, etc. as boundary conditions.
- Data assimilation schemes: the MERRA employs GSI, a 3D-Var data assimilation system which is coupled to the Community Radiative Transfer Model (CRTM) to assimilate radiance observation. LETKF is an ensemble based data assimilation algorithm. It is used to assimilate simulated conventional and retrieval observations in this study.

- Observing systems: the MERRA assimilates real observations, including conventional data, historical radiosonde, and satellite radiance, etc. Millions of observations are assimilated in each 6-hour analysis cycle. Appendix B of Rienecker et al. 2011 provides a complete list of observations used in the MERRA production. While SPEEDY-LETKF is an idealized analysis system assimilating the simulated conventional and retrieval observations generated by adding given errors to a "nature" run. The assimilated observation number is up to 17000 per 6-hour analysis cycle.
- Computational cost: because of the huge amount of observations and the large model size, running the MERRA analysis is computationally quite expensive. The MERRA takes about 2.5 hours for one-day assimilation using NASA's Discover system, while SPEEDY-LETKF takes about 1.5 minutes using UMD AOSC's Atlantic system.

3.2 Hypothesis

We are testing several homogenization strategies using SPEEDY-LETKF system in this chapter. First are two correction methods that use analysis increment differences to change model tendencies, i.e., the MERRA method and the DKM2007 method. We hypothesize that the DKM2007 method will perform better than the MERRA method in minimizing the unwelcome "jump" in SPEEDY-LETKF analysis time series caused by adding AIRS observation, because the correction defined by the MERRA method has been modified by climatological bias between the forecasts of RaobAirs and Raob analyses (Equation (3.9)). By contrast, this background bias is cancelled out

in the DKM2007 method (Equation (3.8)). We also hypothesize that the climatological correction performed *a posteriori* (suggested by B. Hunt, 2012) can also improve the SPEEDY-LETKF but perhaps not as well as the DKM2007 method. Equations (3.8) to (3.10) illustrate the DKM2007 method, the MERRA method, and the climatological correction performed *a posteriori*.

$$Correction(\text{DKM2007}) = \overline{(A_M^M - F_M^M)} - \overline{(A_M^N - F_M^M)} = \overline{(A_M^M - A_M^N)} \quad (3.8)$$

$$Correction(MERRA) = \overline{(A_M^M - F_M^M)} - \overline{(A_N^N - F_N^N)} = \overline{(A_M^M - A_N^N)} - \overline{(F_M^M - F_N^N)} \quad (3.9)$$

$$Correction(climatological) = \overline{A_M^M - A_N^N}, \; then \; \widehat{A_N^N} = A_N^N + \overline{A_M^M - A_N^N} \quad (3.10)$$

In the MERRA system, A_M^M and F_M^M are the analysis and forecast from the MERRA; A_N^N and F_N^N are the analysis and forecast from the NoSSMI; and A_M^N is the analysis whose forecasts start from the MERRA reanalysis 6 hours before current time but no SSM/I observation in analysis process. In the SPEEDY-LETKF system, A_M^M and F_M^M are the analogs of the analysis and forecast from RaobAirs; A_N^N and F_N^N are the analogs of the analysis and forecast from Raob; and A_M^N is the analog of the analysis whose forecasts start from RaobAirs analysis 6 hours before current time, but no AIRS observation. It is clear from (3.8) and (3.9) that the MERRA approach introduces a spurious additional term, the differences in the background forecasts associated with the accumulated past assimilation of SSMI.

3.3 Experiment design

3.3.1 Observing System Simulation Experiments (OSSE)

All experiments conducted in this chapter are OSSEs. In an OSSE framework, observations with prescribed errors are drawn from a "nature run", or the "truth". In our experiment, the "nature run" comes from a coupled SPEEDY-NEMO (Nucleus for European Models of the Ocean) forecast, which was kindly provided by Travis Sluka, who is a Ph.D student of my Department. The SPEEDY version used by Travis is 41, different from the Version 32 used for data assimilation. The horizontal resolutions are the same but the "nature run" has 8 vertical levels instead of 7. In addition, the SPEEDY V41 used as nature is coupled with the NEMO ocean model, which has significant impacts on the model climatology. So our SPEEDY-LETKF is not an "identical-twin", or "perfect-model" analysis system which would not serve our purposes. Schematic figure 3.1 shows the bias between an atmospheric model attractor (red dashed) and the real atmospheric attractor (blue shaded). Since a "perfect-model" has the same climate of "nature", the "jumps" introduced by adding new observations, do not exist. That's why we have to use an imperfect SPEEDY-LETKF in the OSSE experiments. The prescribed observation errors are shown in Table 3.2.

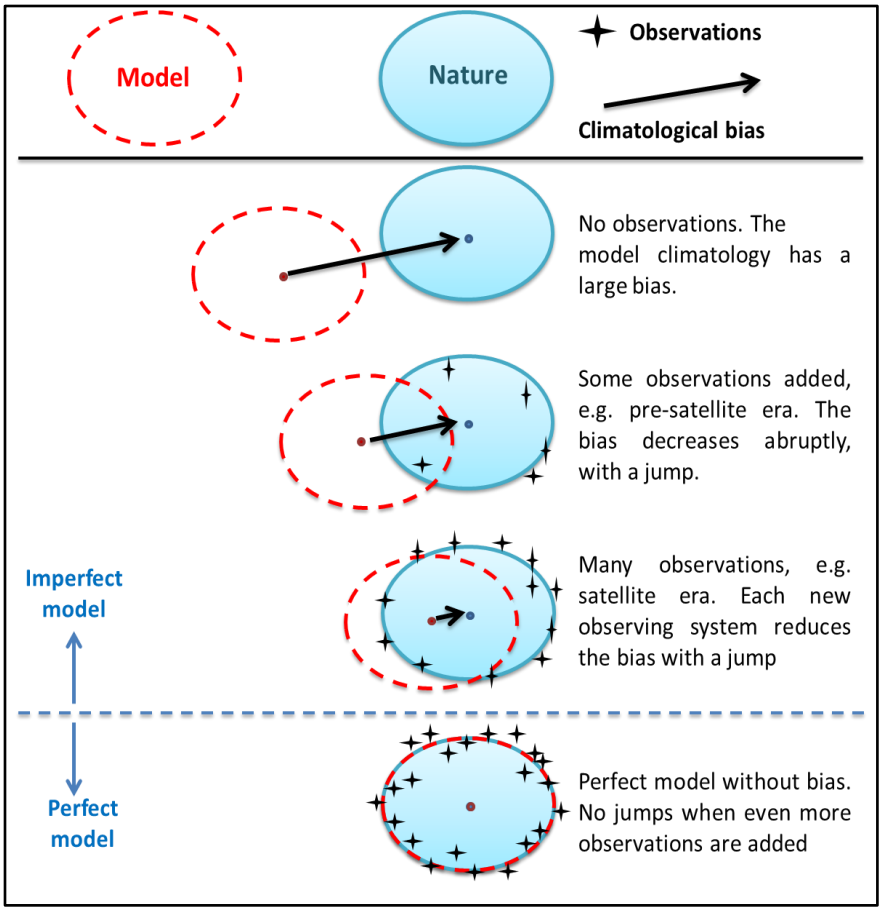

Figure 3.1 A schematic of "climate jumps" associated with observing system changes. Note that there are no jumps when observations are added with a perfect model because the model and the "nature" have the same climatology.

Variables	Observation errors
U	1.0m/s
V	1.0m/s
T_raob, T_airs	1.0K
Q_raob, Q_airs	10^{-3}kg/kg
Ps	1hPa

Table 3.2 The observed variables and their prescribed errors.

3.3.2 Analysis increments approaches

Experiment scenarios. In the MERRA system, the correction terms are computed by the analysis increment differences between the MERRA and the NoSSMI reanalyses. In the SPEEDY-LETKF system, RaobAirs analysis is the analog of the MERRA reanalysis, Raob analysis is the analogy of the NoSSMI reanalysis, and RaobAirs_noAirs is an analysis whose forecasts start from RaobAirs 6 hours before current time with no AIRS observation assimilation.

Following the MERRA method, the analysis increment difference in U, V, T, Q and log(Ps) fields is the comparison between RaobAirs and Raob analyses, denoted by delta_Xai(1), where X represents any combination of themodel variables, U, V, T, Q and/or log(Ps). Following the DKM2007 method, the analysis increment difference is the difference between RaobAirs and RaobAirs_noAirs experiments, denoted by delta_Xai(2) (Table 3.3). Next step is to generate correction terms by applying Fourier transform in time dimension to either delta_Xai(1) or delta_Xai(2) at every grid point. Truncation is the second Fourier terms. The correction terms are then added to SPEEDY model tendency equations. The Raob analyses using modified tendencies are respectively referred to as “debiased (MERRA method)” or “Debiased (DKM2007 method)”, depending on which correction definition method is used. We had tried many combinations of U, V, T, Q and/or log(Ps), like T and Q only, U, V, T and Q, etc. However, the best improvement is achieved when correcting all fields

simultaneously. So we will only show the results from the experiments correcting U, V, T, Q, and log(Ps) together.

Experiment name	Observing Systems	Correction Term Definition
RaobAirs	RAOB, AIRS	**MERRA method** delta_Xai(1) = AI(RaobAirs) – AI(Raob) **DKM2007 method** delta_Xai(2) = AI(RaobAirs) – AI(RaobAirs_noAirs) • X can be either combination of U, V, T, Q and log(Ps)
Raob	RAOB	
RaobAirs_noAirs	RAOB	

Table 3.3 SPEEDY-LETKF Experiment Scenarios

Training period. Considering the error growth of moisture during the first 3 months, our SPEEDY-LETKF experiments, i.e., RaobAirs, Raob, and RaobAirs_noAirs, start from 01/01/1982 but January – March 1982 would be considered as spin-up (we note that we should have taken 6 months rather than 3 months as spin-up, Fig. 3.3). The training period ranges from April 1982 to March 1984. This 2-year long, 6-hourly dataset is then averaged at the corresponding time of the year to create a 1-year long, 6-hourly dataset. Then, Fourier transform is applied. *The analysis to be corrected is a Raob experiment starting from 01/01/1984 with January – March 1984 as spin-up*. Corrections calculated from the training period are added to this biased analysis since April 1984.

Initialization. All SPEEDY-LETKF analyses are initialized with the same background ensembles, which are created by randomly choosing 20 forecasts from "nature run". So the initial background ensembles are very different from the "truth". We note that random forecasts from an imperfect model reanalysis, would have been more realistic (since in reality we do not know nature and have only access to reanalyses) and would have avoided the sudden initial reduction of errors in our results).

3.3.3 *A posteriori* correction

A climatological bias correction performed *a posteriori* (Equation (3.10)) is also investigated (B Hunt, pers. comm., 2012). First, we average the differences of U, V, T, Q, Ps and Rain fields between RaobAirs and Raob experiments during training period, i.e., April 1982-March 1984, at the corresponding time of the year. This generates a 1-year long, 6-hourly datasets. Then a 30-day running mean is conducted in order to remove large day-to-day variability. The smoothed time series are used as climatological correction terms and added to April 1984-March 1985 segment of the biased Raob analysis we aim to correct, at the corresponding time of the year, in the corresponding fields.

3.4 Results

The results of SPEEDY-LETKF experiments are present below, including those from perfect OSSEs, imperfect OSSEs, and a climatological bias correction performed *a posteriori.*

3.4.1 Performance of the perfect SPEEDY-LETKF systems

In the perfect model experiments, "nature run" is created by SPEEDY V32 forecast and thus no model error need to be considered. In order to study the impacts of ensemble member size, we conduct three perfect SPEEDY-LETKF OSSEs assimilating RAOB only. They start from 01/01/1982, with 10, 20, and 50 ensemble members respectively. Their monthly mean precipitation distributions of January 1983 are shown in Figure 3.2. The January 1983 mean precipitation from the 10-member perfect SPEEDY-LETKF analysis (left panel) is not smooth, which indicates that the ensemble size is too small to statistically represent background error. With ensemble size 20 (center panel) and 50 (right panel), the spatial distributions of monthly mean precipitation resemble each other (and show the presence of spectral rain, chapter 4). The differences between 20- and 50- member analyses in U, V, T, Q, and Ps are very small, too (not shown). Thus, we believe that using 20 members is enough to achieve a good data assimilation system.

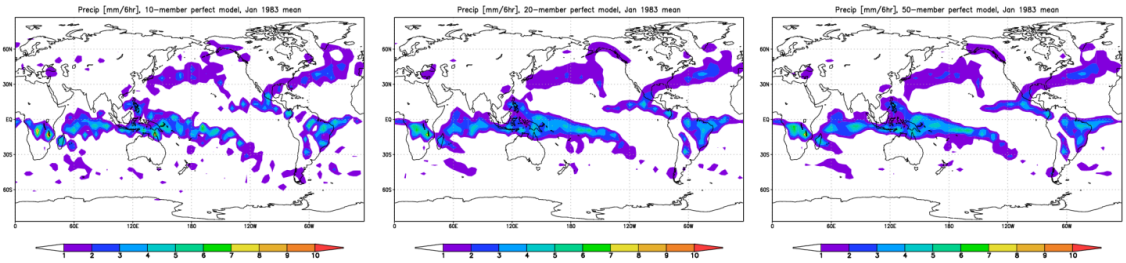

Figure 3.2 January 1983 mean precipitations from perfect member SPEEDY-LETKF analyses with 10- (left), 20- (center), and 50-member (right) respectively.

3.4.2 Performance of the imperfect SPEEDY-LETKF systems

Using the imperfect model SPEEDY-LETKF system, the RaobAirs, Raob, and RoabAirs_noAirs experiments are conducted during the training period. Figure 3.3 shows the Global RMSE of these experiments' outputs at the lowest model level, with U (upper left), V (upper right), Q (middle left), and T (middle right) at 925hPa, Ps (lower left), and precipitation (lower right). Blue represents Raob, red represents RaobAirs, and green represents RaobAirs_noAirs. All three experiments are stable during the training period. The RaobAirs is better than Raob in every variable field, which is reasonable since more observations are assimilated. The RaobAirs_noAirs results are closer to RaobAirs rather than to Raob, which illustrates that the background of has greater impact than observations in this SPEEDY-LETKF system. The results from RaobAirs and RaobAirs_noAirs at 925hPa are almost identical except for Q and T fields. At other model levels, the results from these two analyses are not distinguishable for all multiple level variables, i.e., U, V, Q, and T (not shown).

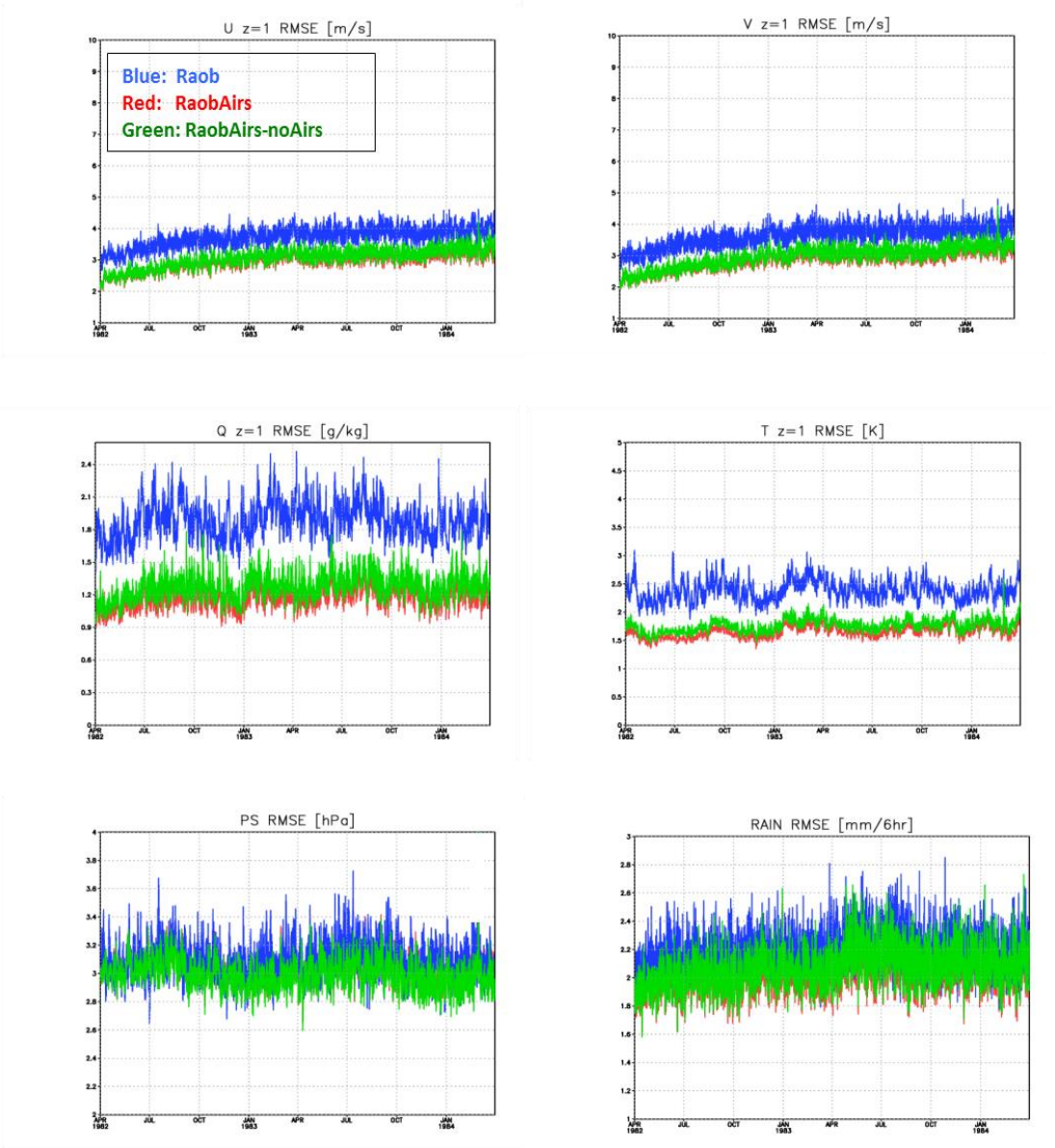

Figure 3.3 Global RMSE of U (upper left), V (upper right), Q (middle left), and T (middle right) at 925hPa, Ps (lower left), and precipitation (lower right), using the stable imperfect SPEEDY-LETKF system with the TRUNCT filter and no-negative-humidity modification. Blue: Raob, Red: RaobAirs, and Green: RaobAirs_noAirs.
Training period: Apr 1982 – Mar 1984

The 1984 summer (JJA) wind stream Altitude-Latitude cross-section at Longitude 180^{O} from RaobAirs experiment (left) and Raob experiment (right) is shown in Figure 3.4. This figure indicates that the Hadley and Ferrel cells do not change significantly without AIRS observation assimilation.

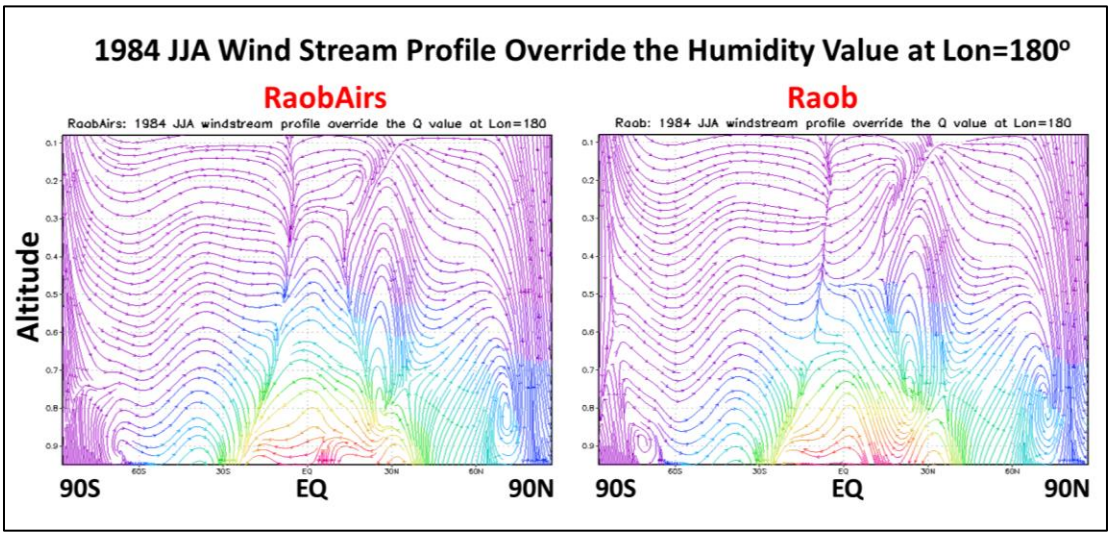

Figure 3.4 Wind stream Altitude-Latitude cross-section at Longitude 180^{O} from RaobAirs experiment (left) and Raob experiment (right). 1984 JJA

3.4.3 Analysis increments

Before introduction into SPEEDY model tendency, we apply Fourier transform to the analysis increment difference, defined by either the MERRA or the DKM2007 method, in order to reduce sampling error, as we did in Chapter 2. Figure 3.5 shows the analysis increment difference of temperature (defined by DKM2007 method) in July (left column) and its corresponding Fourier transfer combining annual mean, semi-annual, and seasonal oscillations (right column) at 200hPa (1st row), 500hPa (2nd row), and 925hPa(3rd row). This figure illustrates that the limited Fourier series truncation is sufficient to represent reasonably well the observed temperature analysis increment difference between RaobAirs and RaobAirs_noAirs experiments. This is also true for other variables defined by either MERRA or DKM2007 method (not shown).

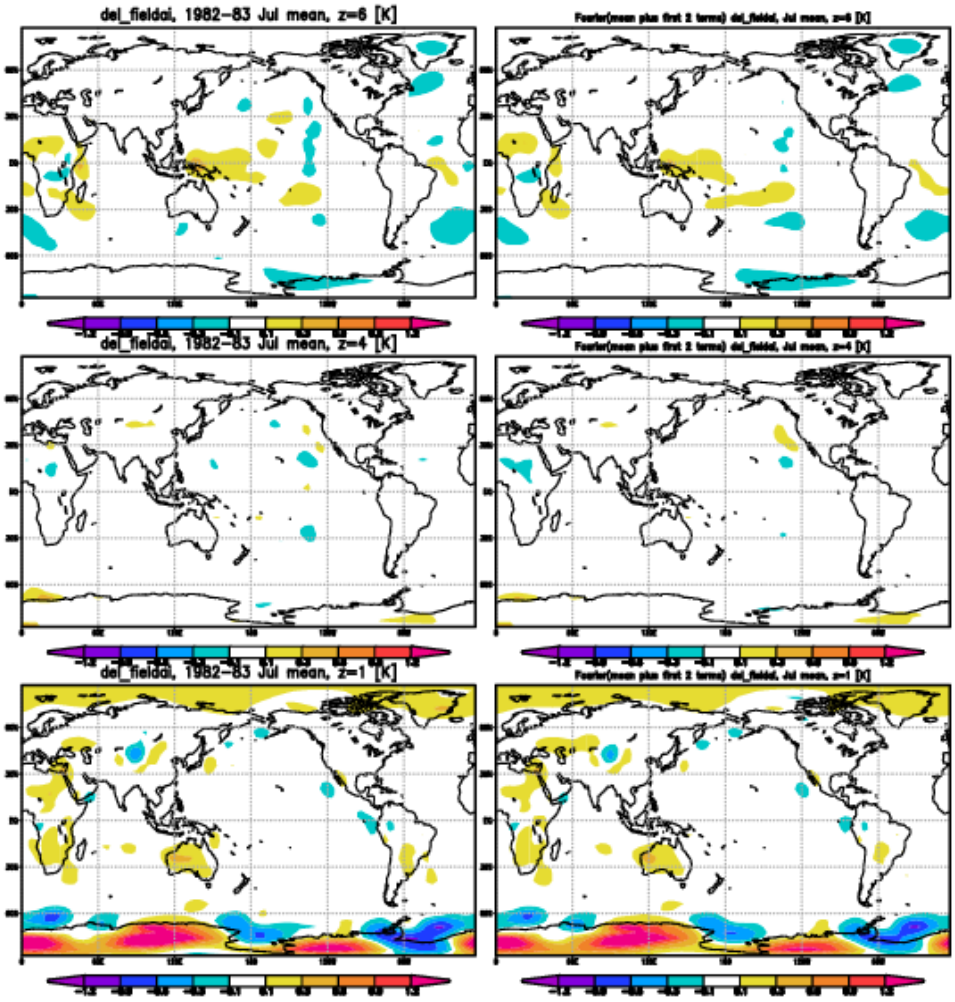

Figure 3.5 July mean of Temperature correction defined by DKM2007 method (left) and its Fourier transform combining annual mean, semi-annual, and seasonal oscillations (right), at 200hPa (1st row), 500hPa (2nd row), and 925hPa(3rd row).

3.4.4 Results from debiased analyses

In an operational system like MERRA, the "truth" or "nature run" is unknown, so we compared NoSSMI reanalysis and its debiased counterparts with MERRA reanalysis in Chapter 2. Likewise, in the SPEEDY-LETKF system, The Raob analysis and all debiased analyses are compared with the RaobAirs analysis rather than to the "nature run". This is because in reality we do not have access to "nature, so that our goal is to

minimize the climate jumps between RaobAirs (our best analysis with the most complete observing system), and the Raob analyses before the introduction of the AIRS observing system.

Figure 3.6 shows the specific humidity deviations with respect to RaobAirs for 1984 July average, with the 1st column representing the Q deviation from the Raob experiment, the 2nd column the debiased (MERRA method) experiment, the 3rd column the Debiased (DKM2007 method) experiment, and the 4th column the climatological bias correction method. The analysis of Q is turned off at the higher levels, so only the humidity lower than 500hPa are shown in this figure. The 1st row 500hPa, and the 2nd row 925hPa. All debiased analyses overcorrect specific humidity of the Raob analysis at 200hPa level. At 925hPa, the debiased (MERRA method) analysis reduced the deviation over the Arctic, the Debiased (DKM2007 method) analysis reduced the deviation over the Tropics, and the climatological bias correction analysis overcorrects the Raob analysis over the Tropics and the extratropical region. Figure 3.7 is similar to Figure 3.6 except that it is for temperature at three levels. All debiased experiments improve the Raob analysis at all levels, while the Debiased (DKM2007 method) is the optimum. The debiased (DKM2007 method) analysis reduces the deviation significantly at 200hPa, over the Antarctic and the southern Pacific Ocean and the southern Atlantic Ocean.

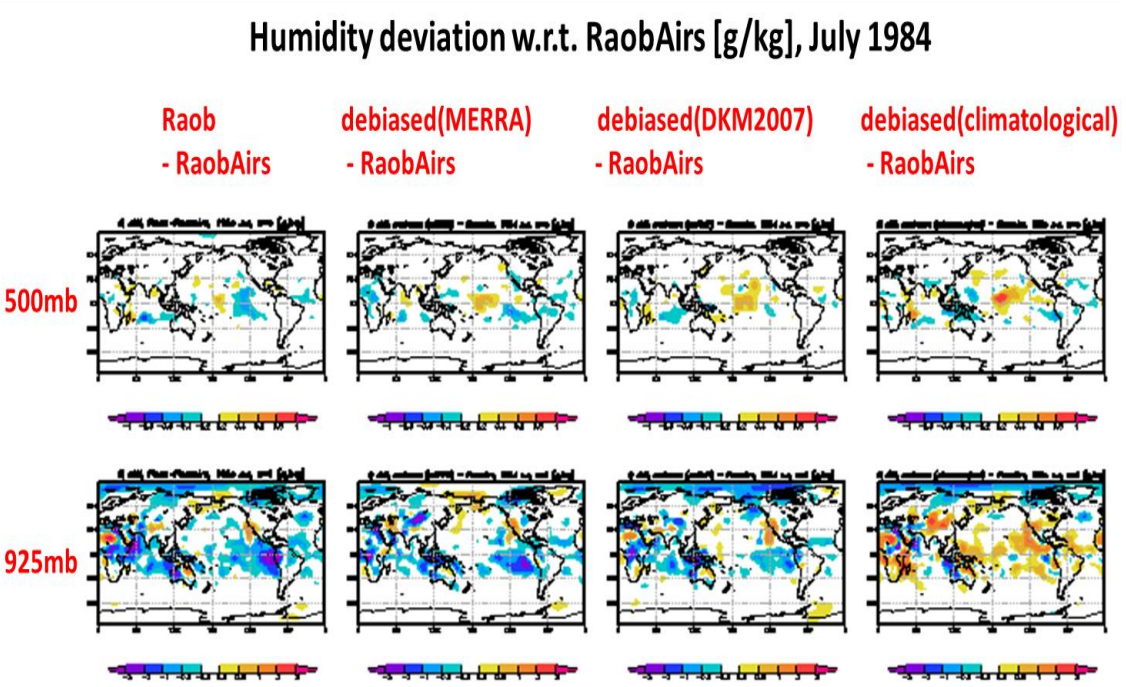

Figure 3.6 The specific humidity deviations w.r.t RaobAirs for 1984 July average, with the 1st column represents Q deviation from the Raob experiment, the 2nd column the debiased (MERRA method) experiment, the 3rd column the debiased (DKM2007 method) experiment, and the 4th column the climatological bias correction method. The 1st row represents 500hPa, and the 2nd row 925hPa. [g/kg]

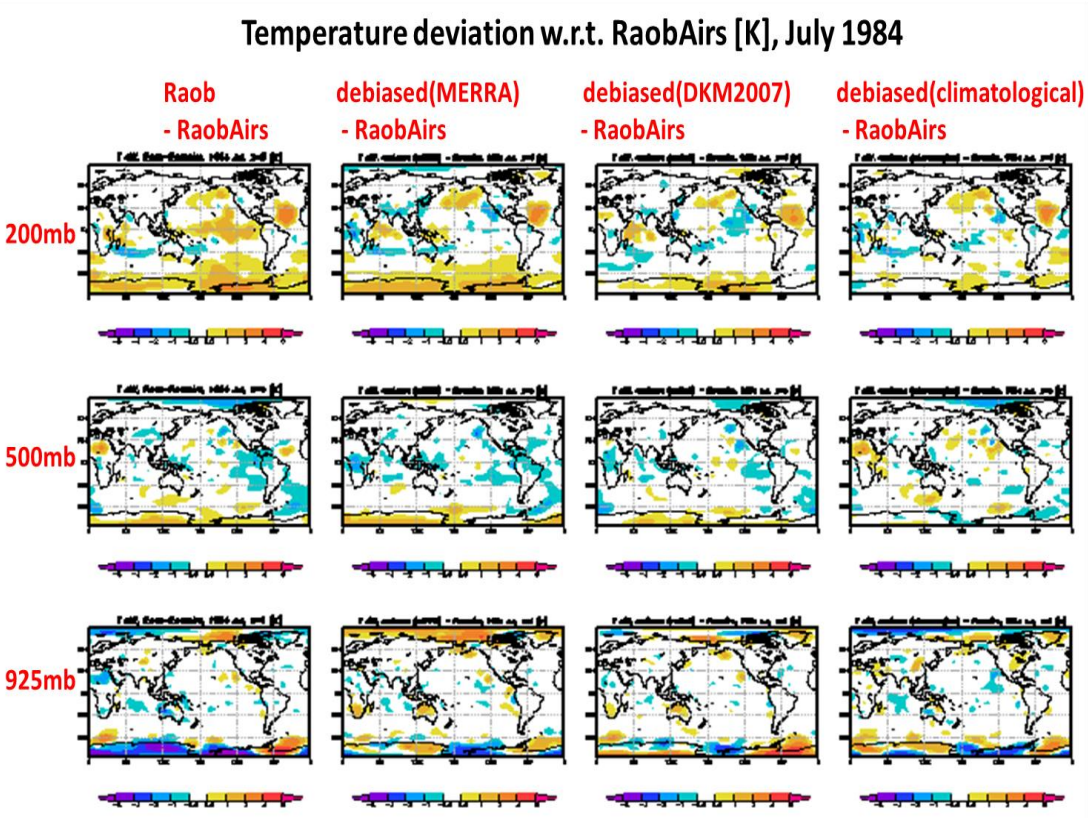

Figure 3.7 Similar to Figure 3.6, but for temperature at 3 levels.[K]

Figures 3.8 shows the 1984 July profiles of deviations (dashed lines) and RMSDs (solid lines) for Q (upper left), T (upper right), U (lower left), and V (lower right) from the Raob analysis and all debiased analyses. Red color represents the Raob analysis, green the debiased (MERRA method) analysis, blue the Debiased (DKM2007 method) analysis, and orange the climatological bias correction analysis.

This figure illustrates that, in 1984 July the climatological bias correction method has a tendency to overcorrect the Raob humidity at lower levels, which is also seen on Figure 3.6. The specific humidity RMSDs of debiased (MERRA method) and Debiased (DKMD2007) are smaller than the climatological bias correction method at

the middle-to-lower levels. For temperature, although the mean deviation from the climatological bias correction method is the smallest, the RMSDs of debiased (MERRA method) and Debiased (DKMD2007) are smaller at all levels. For the wind fields, there is almost no difference between the RMSDs from the climatological bias correction and the Raob analyses. And the improvements of both U and V are similar from the debiased models using the analysis increments approaches.

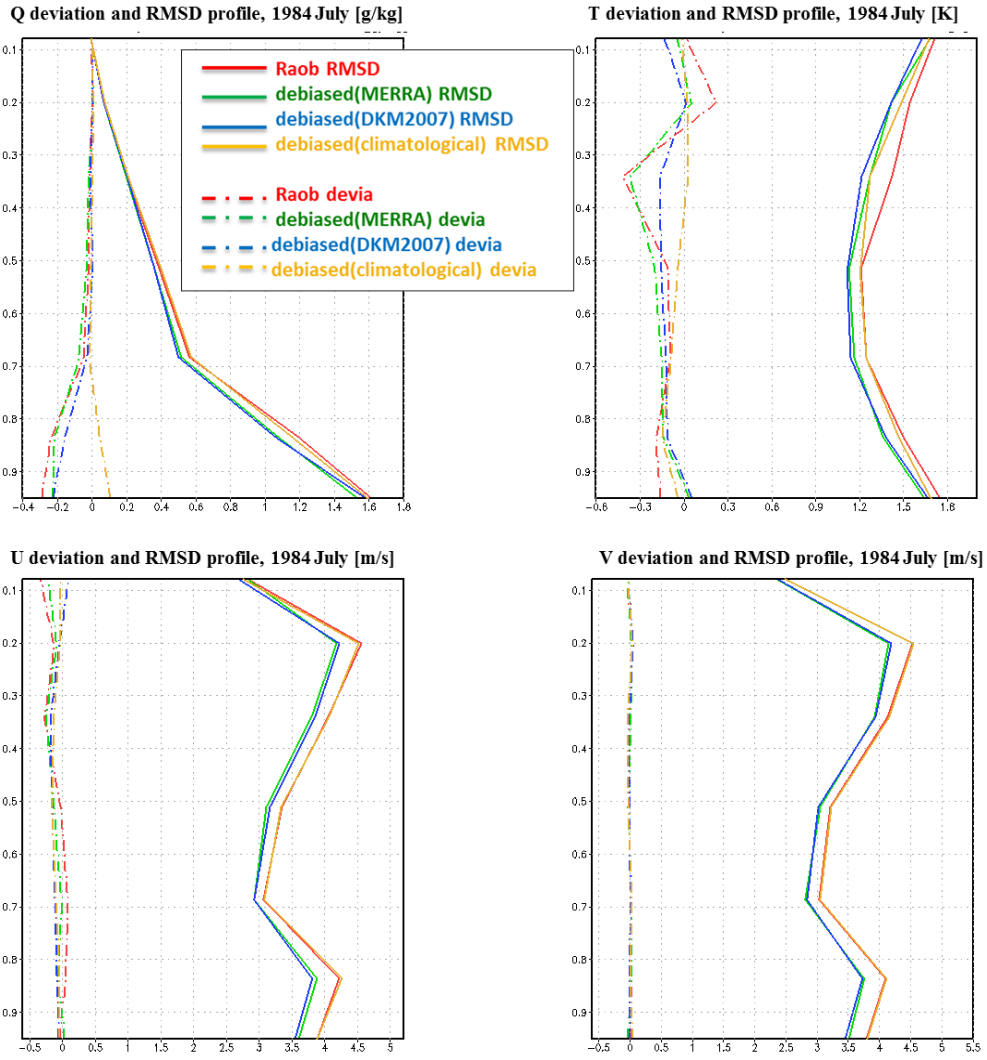

Figure 3.8 Profiles of 1984 July mean deviations (dashed lines) and RMSDs (solid lines) for Q (upper left), T (upper right), U (lower left), and V (lower right) from the Raob analysis (red), the debiased (MERRA method) analysis (green), the Debiased (DKM2007 method) analysis (blue), and the climatological bias correction analysis (orange).

Figure 3.9 is the same as Figure 3.8 but for 1984 December. In December 1984, the improvements of debiased (DKM2007 method) are significant for temperature and winds. The U and V RMSDs from debiased (MERRA method) are the same as the Raob analysis at middle-lower levels. Its Q RMSD is even the worst at higher levels. When comparing Figure 3.8 and 3.9, the DKM2007 method is superior to the MERRA method because the improvement of the former method is more consistent in time.

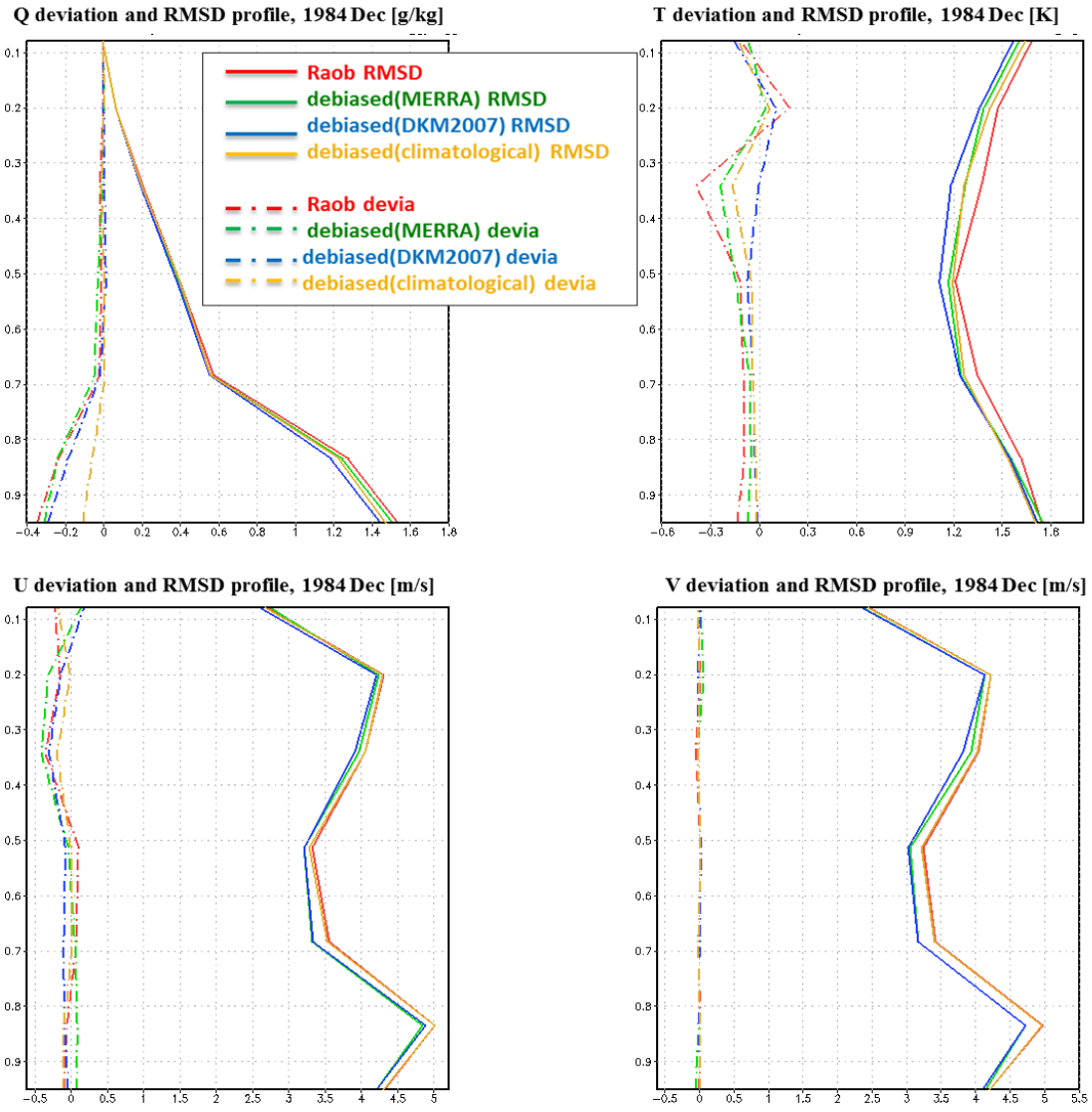

Figure 3.9 The same as Figure 3.8 but for 1984 December.

The impacts of debiased experiments for precipitation are studied by exploring the 9-day running mean of precipitation RMSDs with respect to RaobAirs (Figure 3.10), during May 1984 to Mar 1985. Red line represents RMSD from the Raob analysis, green the debiased (MERRA method) analysis, blue the debiased (DKM2007), and orange the climatological bias correction analysis. The time averaged RMSD values over this time period are given by the figure legend, with 2.22 for Raob analysis (red), 2.16 for debiased (MERRA method) analysis (green), 2.13 for dDebiased (DKM2007 method) analysis (blue), and 2.23 for climatological bias correction analysis (orange). The climatological method fails to correct Raob analysis, and the debiased (DKM2007 method) analysis shows most significant improvement. The debiased (MERRA method) analysis is doing well from May to October 1984, but its error grows up since November 1984 and even becomes greater than the uncorrected Raob analysis from mid-November to mid-January 1985. The precipitation RMSD difference between debiased (DKM2007) and debiased (MERRA) is shown in Figure 3.11. The horizontal dashed line in the middle of this figure is value ZERO. It is obvious that the DKM2007 method outperforms the MERRA method during May 1984 to March 1985. It is interesting to observe that, the debiased (DKM2007) and the debiased (MERRA) analyses gradually merge to the Raob analysis. We believe that this is because we set negative humidity values to zero and thus added humidity source to the system. So the precipitation error grows in long-term runs.

Table 3.4 shows horizontally-averaged Monthly RMSD differences for Q, T, U, and V between debiased(DKM2007) and other analyses. The RMSDs from the

debiased(DKM2007) are always smaller than those from other debiased reanalyzed. This is statistically significant when tested by a paired t-test at 5% level.

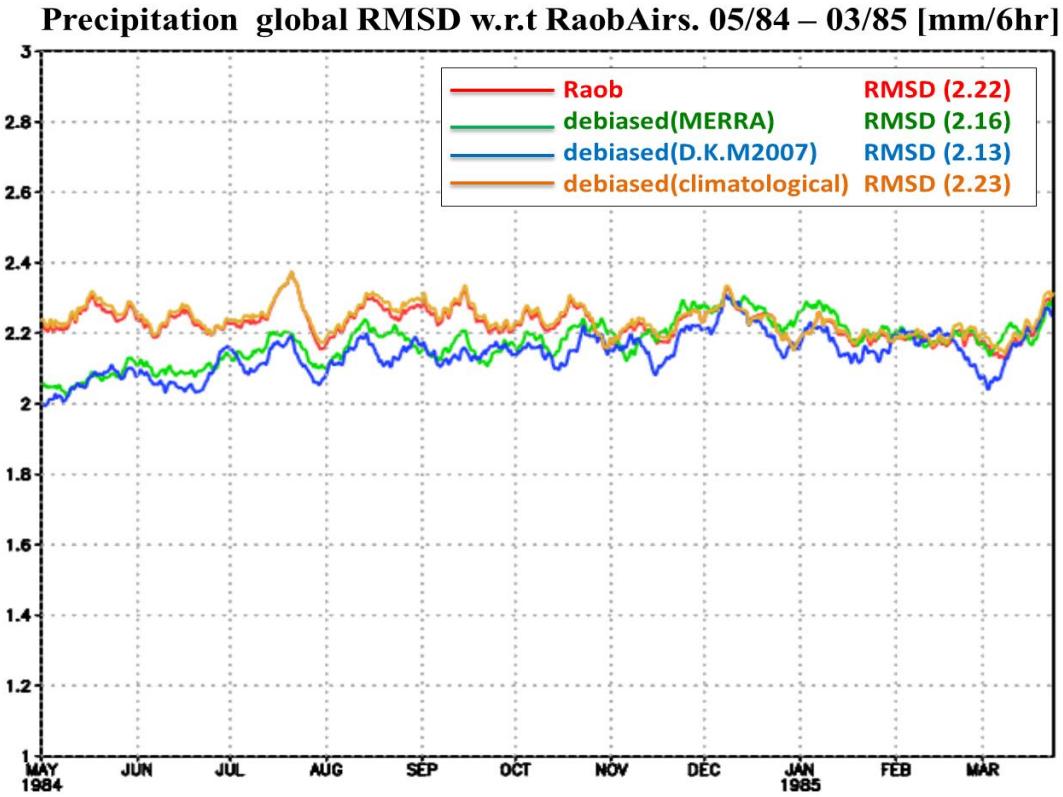

Figure 3.10 Precipitation global RMSD time series with respect to RaobAirs analysis, during May 1984 to March 1985. The time averaged RMSD values over this time period are **2.22** for Raob analysis (red), **2.16** for debiased (MERRA method) analysis (green), **2.13** for debiased (DKM2007 method) analysis (blue), and **2.23** for climatological bias correction analysis (orange).

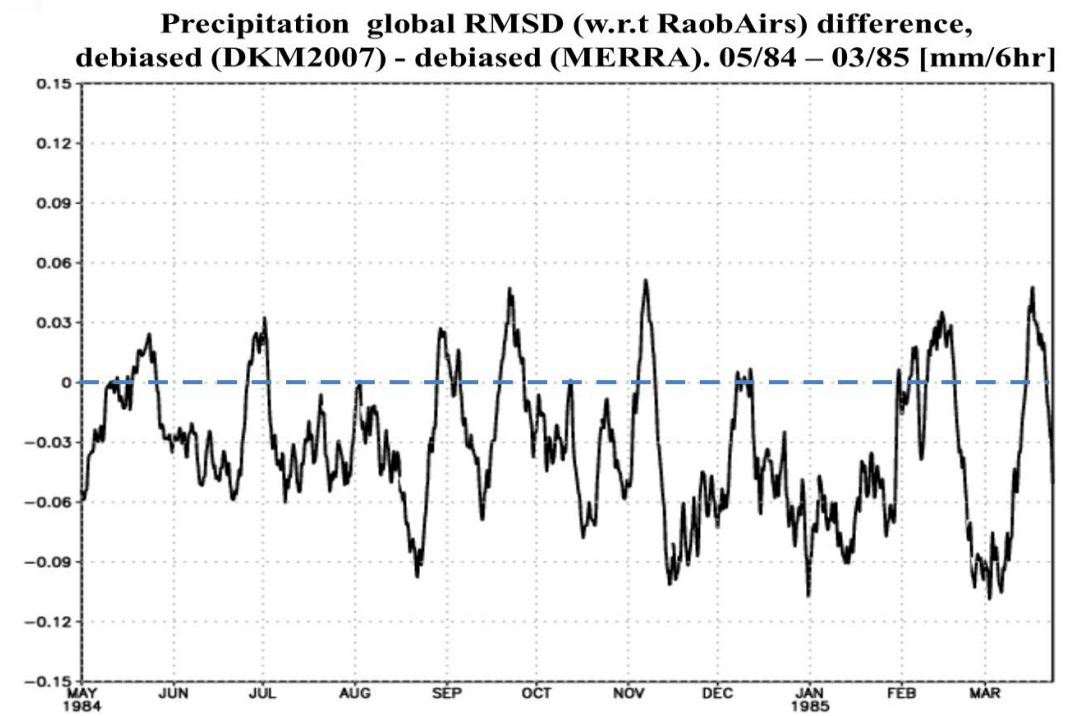

Figure 3.11 Precipitation global RMSD (with respect to RaobAirs analysis) difference, debiased (DKM2007) - debiased (MERRA).05/84-03/85 [mm/6hr]. The horizontal dashed line in the middle of the figure is the value ZERO.

RMSD differences	Q[g/kg]	T[K]	U[m/s]	V[m/s]
debiased(DKM2007)-RAOB	-0.03	-0.07	-0.14	-0.15
debiased(DKM2007)-debiased(MERRA)	-0.01	-0.03	-0.06	-0.04
debiased(DKM2007)-debiased(climatological)	-0.02	-0.05	-0.15	-0.16

Table 3.4 Horizontally-averaged Monthly RMSD differences for Q, T, U, and V.

3.5 Conclusions for Chapter 3

In Chapter 3, we explore three strategies to minimize the climate jumps in an analysis introduced by adding new observing systems. The data assimilation system used in present chapter is the imperfect SPEEDY-LETKF OSSE.

The first strategy resembles the MERRA experiments described in Chapter 2, denoted by MERRA method. The counterpart of the MERRA (the NoSSMI) reanalysis is the RaobAirs (the Raob) analysis. Our goal is to minimize the climatological deviations of the Raob analysis from the RaobAirs analysis. Following the MERRA method, the correction terms are computed by analysis increment differences between the RaobAirs and the Raob analyses. Similar to the conclusions from MERRA experiments in Chapter 2, this method is also only partially successful. This method succeeds in minimizing "climate jumps" for Q, T, U, V, and precipitation fields during the first 7 months of the debiased experiment period (1984 April - October). However, the improvements disappear and the errors of the debiased (MERRA method) analysis grow up starting in mid-November. We conclude that the analysis increment differences between the RaobAirs and the Raob are not just due to the assimilation of AIRS, but to the nonlinear interactions between the variables currently observed by AIRS, and the variables that have been modified by previous assimilations of AIRS. These nonlinear interactions would introduce accumulated impacts during the 2-year experiment period.

In order to minimize the nonlinear interactions, we conduct a SPEEDY-LETKF experiment whose forecasts start from the RaobAirs analysis while assimilates RAOB only, denoted by RaobAirs_noAirs. So the RaobAirs and the RaobAirs_noAirs analyses have the same background but different observing systems. The analysis increment differences between them are assumed to be linear within each 6-hour analysis cycle and do not contain the accumulated nonlinear errors during the training period. This strategy is referred to as DKM2007 method. The results from debiased (DKM2007 method) analysis are encouraging. The global T, U, V, and precipitation RMSDs with respect to RaobAirs are always the smallest among all debiased analyses, at almost all levels, and over the whole debiased experiment period. For specific humidity, the main improvement is a significantly smaller deviation at lower levels (925hPa) over the Tropics. For temperature, the main improvements are smaller deviation over the Antarctic and the southern Atlantic Ocean at 200hPa, and over Polar Regions at 925hPa. For precipitation, the debiased (DKM2007 method) analysis dramatically outperforms the other two debiased analyses. This indicates that with better wind and temperature analyses, the SPEEDY-LETKF system is more balanced and its diagnostic precipitation field is also improved.

The climatological bias correction performed *a posteriori* only succeeds in improving temperature at mid and high levels in 1984 July. This strategy overcorrects lower level humidity in 1984 July. For wind fields and precipitation, there is not noticeable benefit from this method.

Chapter 4 Spectral model instability

4.1 Introduction

In a closed system described by the basic meteorological equations, one can expand the dependent variables in terms of a finite series of smooth orthogonal functions, such as Fourier-Legendre functions, in space. The problem now is to solve a set of ordinary differential equations (ODEs) for the coefficients of these functions. These coefficients depend on time and the vertical coordinate, and thus the horizontal spatial dependence is removed. The application of the spectral model was initiated by Silberman in 1954. The advantages include accurate space derivatives, nonlinear quadratic terms computed without aliasing, fewer degrees of freedom required for a given accuracy than in a grid point model, and that the model is computationally more efficient (Riddaway et al. 2011). It has become more popular for numerical weather forecasts and general circulation research at the operational and academic institutes for the past several decades (Krishnamurti 2006).

However, there are some artifacts when representing positive value variables in spectral model, such as orography (Lindberg 1996), surface pressure (Baek 2009), and humidity (Figure 4.1). The finite truncation in spectral space may cause overshoots or undershoots of the orthogonal function sums at a jump discontinuity, and the overshoots do not die out as the frequency increases. This is known as Gibbs phenomenon, which may generate negative values in physical humidity field locally. This phenomenon is especially bothersome for humidity because it is involved in

physical parameterization schemes (Royer 1986). Local negative values of humidity could be corrected by setting the negative values to zero, "borrowing" nearby positive values, or by conserving the global amount of water, etc.

The SPEEDY V32 used in the SPEEDY-LETKF system is a low resolution spectral model. The negative humidity values are generated from SPEEDY forecast at the top 3 levels. For example, Figure 4.1 shows the specific humidity mean of July 1982 from SPEEDY V32, at sigma level 6 (the second highest level). The cold colors are negative values, and warm colors are positive values. In order to achieve a more stable system, the specific humidity analysis is turned off at these levels.

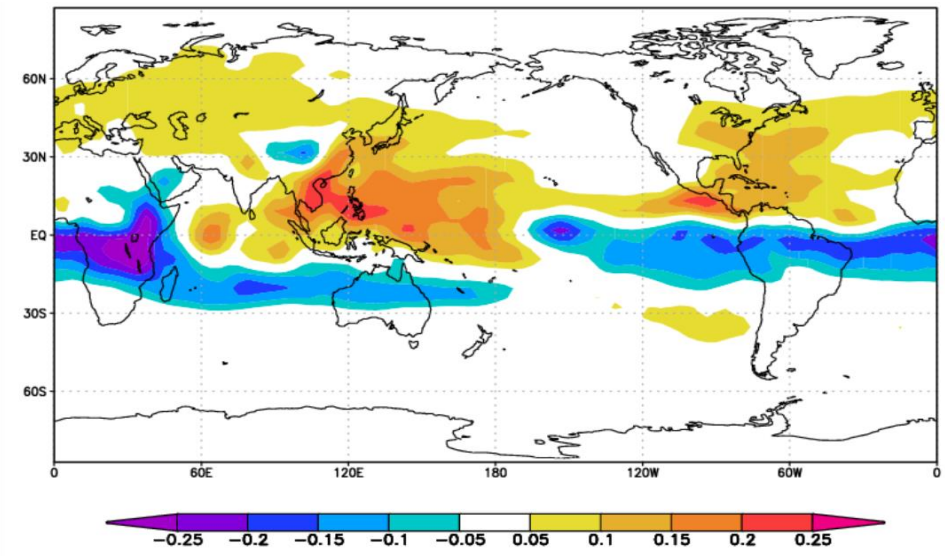

Figure 4.1 Specific humidity mean of July 1982 from SPEEDY V32, at sigma level 6 (the second highest level). Cold colors are negative values, warm colors are positive.

The "Gibbs ripples" clearly present in surface pressure field from SPEEDY-LETKF, as well as other spectral reanalyses such as the NCEP and the ERA15, but since their resolutions are higher than that of the SPEEDY model, their impact is smaller. Figure

4.2 shows the annual average of surface pressures from 20-year climates from SPEEDY (left), NCEP/NCAR Reanalysis (middle), and ERA15(right). This figure was kindly provided by Alfredo Ruiz-Barradas.

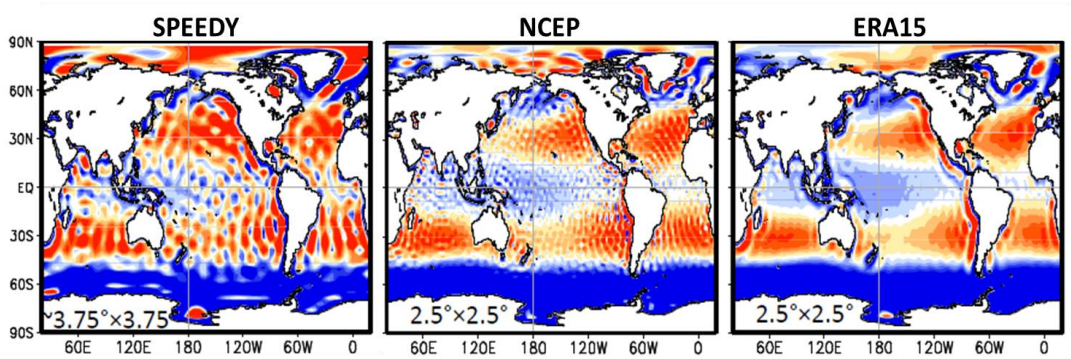

Figure 4.2 Annual average of surface pressures from 20-year climates from SPEEDY (left), NCEP (middle), and ERA15 (right) (courtesy of Alfredo Ruiz-Barradas)

4.2 The instability of the imperfect SPEEDY-LETKF analysis system

In the imperfect SPEEDY-LETKF analysis system, the "nature run" is a long integration from the coupled SPEEDY-NEMO model. So the climate of "nature" is different from that of the SPEEDY V32 used to generate forecasts (the background) in the analysis system, so that model error exists.

One problem of conducting imperfect OSSEs is that the difference between model climate and the "nature run" climate leads to instability in our SPEEDY-LETKF system. The 20-member experiment assimilating only RAOB blows up after about 2 months of integration, because it generates unphysical negative humidity at high latitudes. For example, for a 20-member imperfect RAOB experiment starting from 00Z, 01/01/1982, negative Q began showing up at every model levels after only 10

days analysis. This experiment finally blew up at 18Z, 02/24/1982 with huge negative humidity values appear over the Antarctic, at 925hPa level (Figure 4.3). Large negative humidity values are observed at every model level.

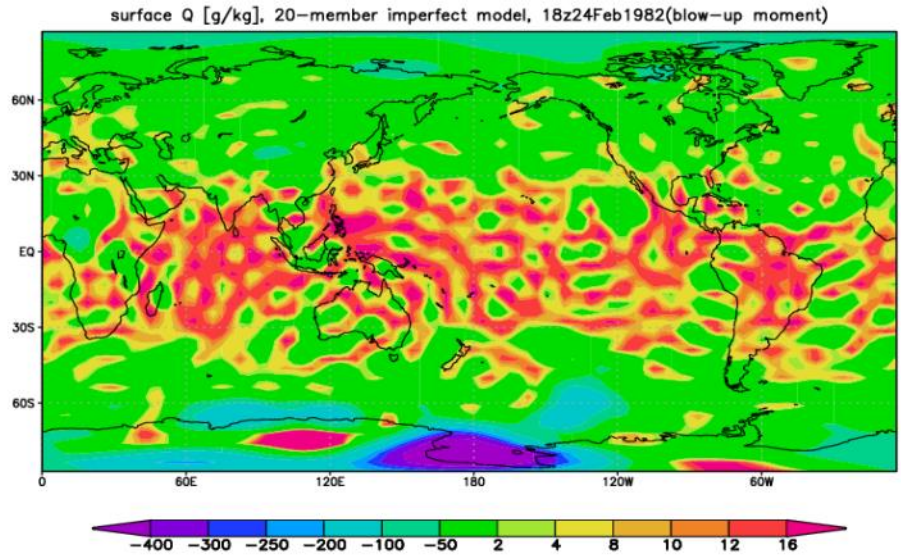

Figure 4.3 Specific humidity from a 20-member imperfect Raob experiment at 18:00Z of February 24th, 1982 (blow-up moment), at 925hPa

Figure 4.4 compares the difference between "nature run" and SPEEDY V32 climates. The 925hPa July means of 4-year experiments for specific humidity is shown on the 1st row and for temperature on the 2nd row, with left represents "nature run" and right represents SPEEDY v32. The model error evolves nonlinearly and accumulates with time, finally leading to model blow-up because of negative humidity (Figure 4.3). The "nature" is hotter and more humid around ITCZ regions in NH summer.

In Chapter 3, we had addressed that increasing ensemble member size can improve the analysis of precipitation and all other fields in a perfect SPEEDY-LETKF system. However, the impact of the ensemble member size is opposite in an imperfect

SPEEDY-LETKF system and made it blow up earlier. For example, the 10-member imperfect SPEEDY-LETKF analysis can run about 13 months, 20-member about 2 months, and 50-member about 1 month.

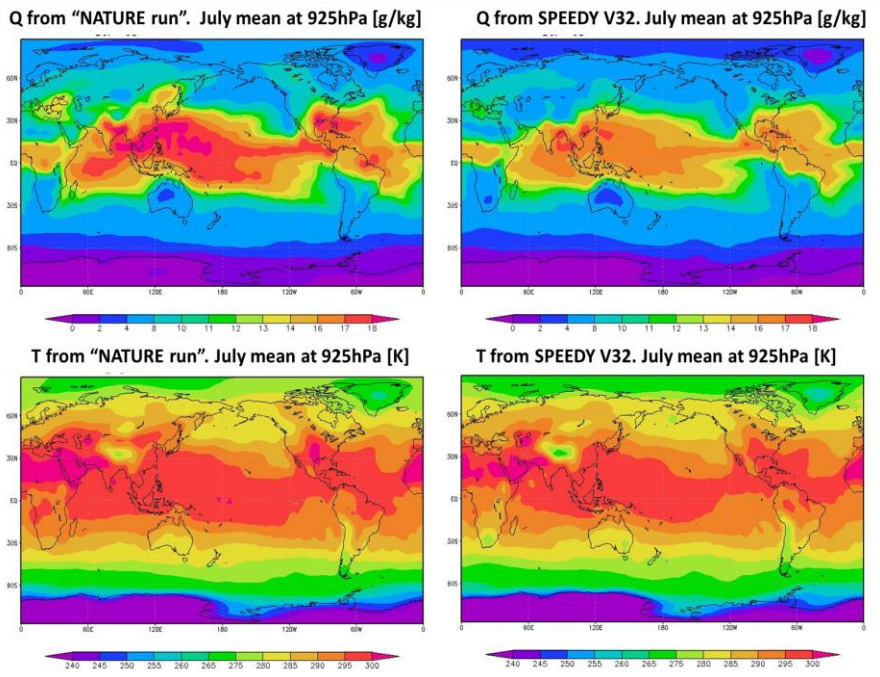

Figure 4.4 The 925hPa July means of 4-year experiments for specific humidity (1st row) and for temperature (2nd row), with "nature run" (left) SPEEDY v32 (right)

4.3 Efforts made to avoid the imperfect SPEEDY-LETKF analysis system blow-up

We made several efforts to correct the model bias and avoid blow-up in the imperfect SPEEDY-LETKF analysis system. For example, we tried the following strategies:

- Setting negative specific humidity values analysis to zero,
- Applying a linear filter to orography and surface pressure in spectral space,
- Applying the Shapiro filter to analysis increment at every 6-hour analysis cycle,

- Changing localization length scale,

- Using both adaptive multiplicative inflation and additive inflation techniques.

Unfortunately, none of these strategies could stabilize the imperfect SPEEDY-LETKF analysis system. The only two stable systems available are

1) Following the suggestion of Kayo Ide and Catherine Thomas (2014), we can stabilize the imperfect SPEEDY-LETKF OSSE by applying a truncation filter that eliminates spectral components outside the triangular truncation (known as TRUNCT filter). K. Ide and C. Thomas pointed out that, in the default SPEEDY model, the TRUNCT filter is only applied to vorticity and divergence during initialization of each 6-hour forecast, and to time tendencies of vorticity, divergence, temperature, log(Ps), and specific humidity at every time step (40 minutes). In our modified system, when initializing every 6-hour SPEEDY forecast and at every time steps (40 minutes per time step) within the 6-hour window, the TRUNCT filter was also applied to vorticity, divergence, temperature, log(Ps), and specific humidity. However, the negative humidity analysis still appears, leading to a blow-up. As a crude solution, we set all negative humidity values at the lowest four model levels to zero, although this adds a humidity source to SPEEDY. We had tested the TRUNCT filtering and no-negative-humidity methods separately. Neither of them alone succeeded in stabilizing the imperfect SPEEDY-LETKF system.

With both of the TRUNCT filter and no-negative-humidity modification, the imperfect SPEEDY-LETKF system becomes stable. This is the system used in Chapter to explore minimization strategies for “climate jumps” in reanalyses.

A drawback of this system is that, when assimilating RAOB only, the global RMSE of 925hPa specific humidity increases during the first 3-6 months of the analysis (Figure 4.5). Therefore, the first 3 month is considered as spin-up period.

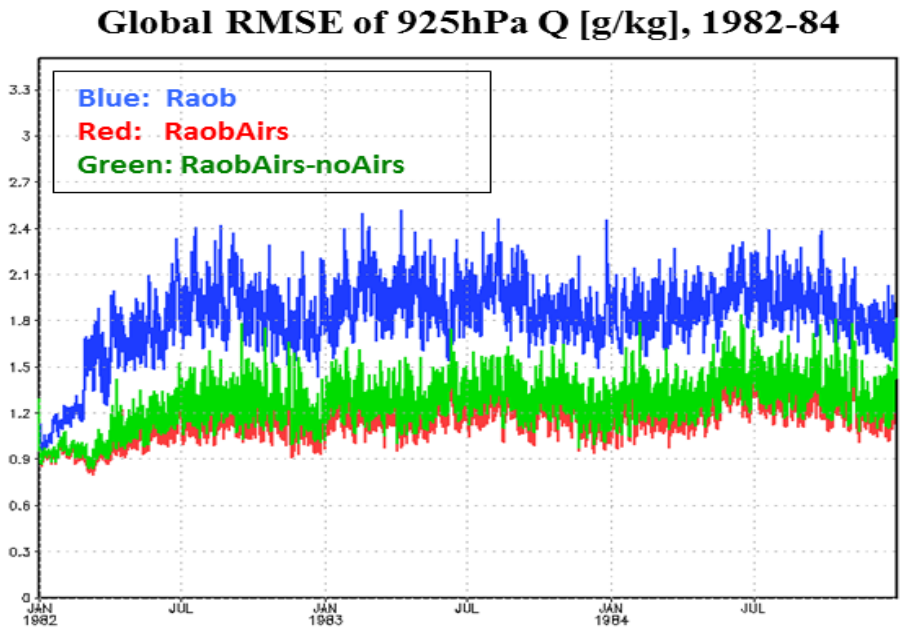

Figure 4.5 Global RMSE of specific humidity at 925hPa, using the stable imperfect SPEEDY-LETKF system with the TRUNCT filter and no-negative-humidity modification. Blue: Raob, Red: RaobAirs, and Green: RaobAirs_noAirs.1982-84

2) not to analyze specific humidity so that the Q analysis is only determined by the SPEEDY forecast. This system will be discussed in Section 4.4

Figure 4.6 shows the 925hPa temperature fields from 20 members imperfect SPEEDY-LETKF systems at 18:00, February 24th 1982 (the default model blow-up moment). Left panel is for the default SPEEDY-LETKF, middle panel for the no-Q-analysis system, and right panel for the TRUNCT filtered system. This figure shows that he "Gibbs ripples" in the temperature fields can be avoided by applying the TRUNCT filter and setting all negative humidity values to zero.

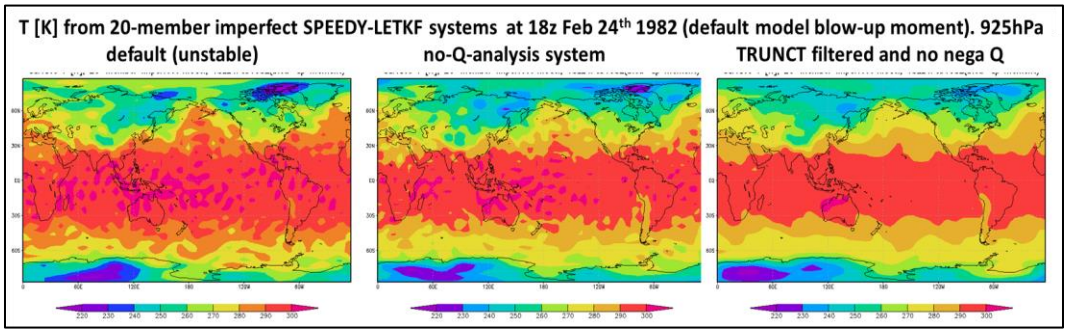

Figure 4.6 The 925hPa temperature fields from 20 members imperfect SPEEDY-LETKF systems at 18:00, February 24th 1982 (the default model blow-up moment). Left panel is for default SPEEDY-LETKF, middle panel for the no-Q-analysis system, and right panel for the TRUNCT filtered system.

4.4 The stable imperfect SPEEDY-LETKF analysis system without specific humidity analysis

The no-humidity-analysis modification increases substantially the RMSE of humidity and temperature. For example, in a one year Raob experiment starting from 01/01/1982 (Figure 4.7), the global RMSE of specific humidity (left panel) and temperature (right panel) at the lowest model level grows up dramatically after the spin-up period (about 10 days), and become stabilized after 3 month integration (blue lines). If doing a RaobAirs experiment, the humidity and temperature global RMSE at

the same level increases much less (red lines). Figure 4.8 shows the 1982 December mean of temperature analysis from the Raob experiment. The "Gibbs ripple" phenomena in temperature field are observed between 30^{o}S~30^{o}N at all levels.

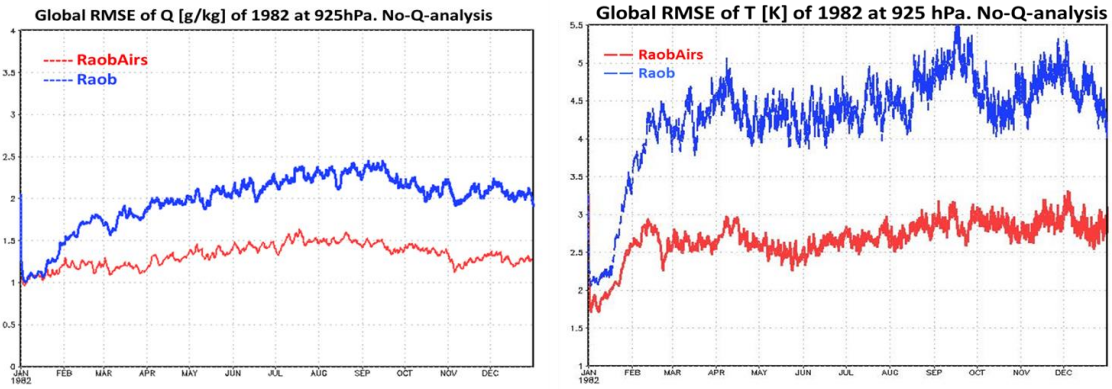

Figure 4.7 Global RMSE of specific humidity (left) and temperature (right) from imperfect SPEEDY-LETKF experiments without humidity analysis for 1982, at 925hPa. RaobAirs analysis is represented by red, and Raob analysis by blue.

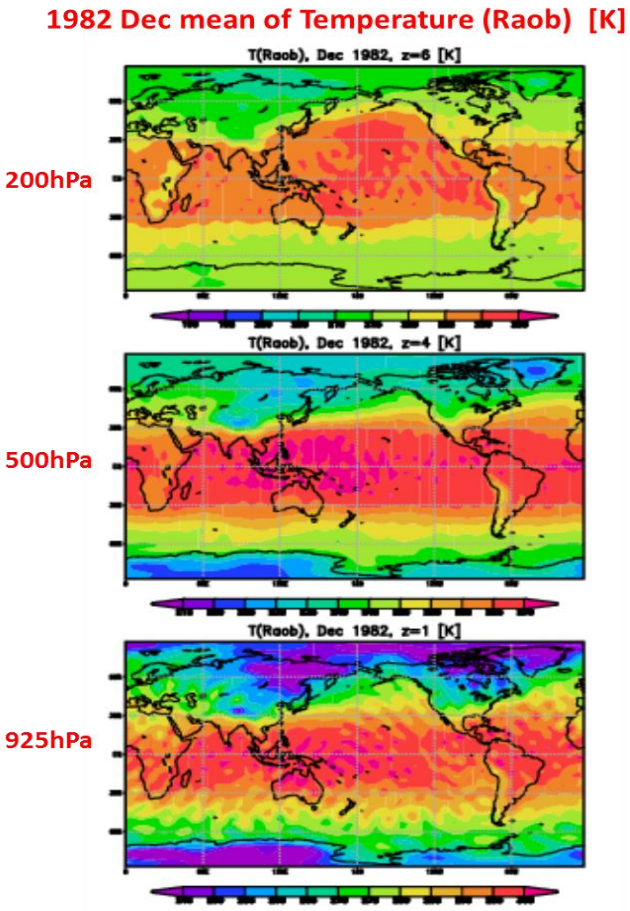

Figure 4.8 December 1982 mean of temperature from imperfect Raob experiments without humidity analysis.

Figure 4.9 shows the July mean of temperature analysis increment difference between the RaobAirs and the Raob analyses (left) and its 2-term-truncation Fourier transform (right), during the training period, from the stable no-humidity-analysis SPEEDY-LETKF system at 200mb (1st row), 500hPa (2nd row), and 925hPa(3rd row). Although "Gibbs ripples" are observed at the lowest model level, the temperature analysis increment difference can be well represented by the 2-term-truncation Fourier transform. This conclusion is true for MERRA reanalysis system and the stable imperfect SPEEDY-LETKF system with the TRUNCT filter and no-negative-humidity output modification.

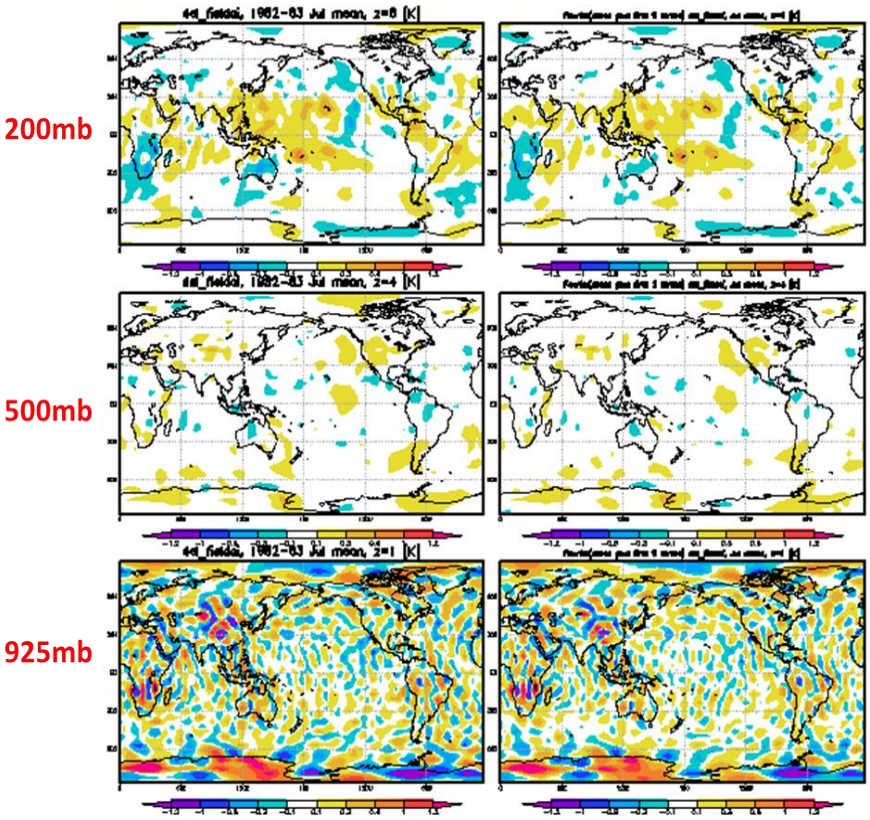

Figure 4.9 July mean of temperature analysis increment difference between the RaobAirs and the Raob analyses (left) and its 2-term-truncation Fourier transform (right), during the training period, from the stable no-humidity-analysis SPEEDY-LETKF system at 200mb (1st row), 500hPa (2nd row), and 925hPa(3rd row). [K]

Since the humidity is not constrained by the observations, the physical parameterization processes based on moisture are not reliable and the SPEEDY-LETKF system is biased. Even though the system does not blow up, the "Gibbs ripples" appear in the temperature field. In order to investigate what would happen if we apply the "climate jumps minimization" strategies described in Chapter 3, the MERRA method, the DKM2007 method, and the climatological correction method are applied to the no-Q-analysis SPEEDY-LETKF analysis system. The result for temperature is shown in Figure 4.10.

Figure 4.10 shows the temperature deviations with respective to RaobAirs for 1984 July average using the stable no-humidity-analysis SPEEDY-LETKF system at 200mb (1st row), 500hPa (2nd row), and 925hPa(3rd row). The 1st column represents T deviation from the Raob experiment, the 2nd column the debiased (MERRA method) experiment, the 3rd column the Debiased (DKM2007 method) experiment, and the 4th column the climatological bias correction method. The debiased (MERRA method) actually increases the bias, the debiased (DKM2007) method does not improve it and the climatological correction overcorrects. We conclude that without assimilation of moisture, the errors become so large that the reanalysis is of unacceptable quality.

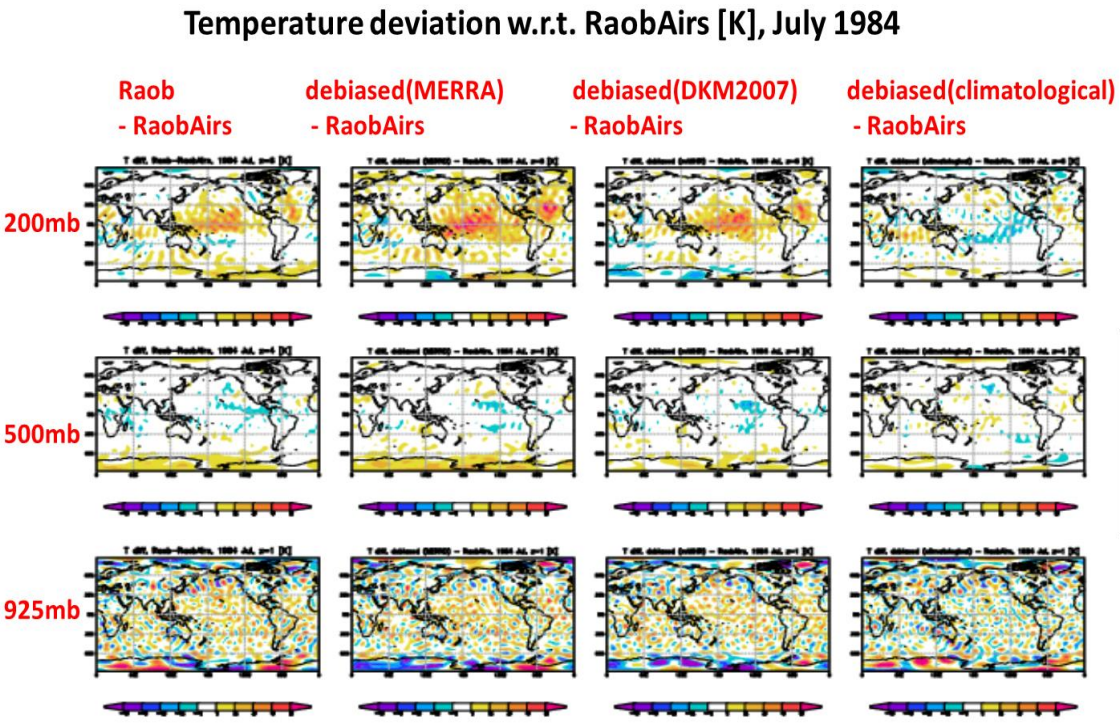

Figure 4.10 The temperature deviations with respective to RaobAirs for 1984 July average using the stable no-humidity-analysis SPEEDY-LETKF system at 200mb (1st row), 500hPa (2nd row), and 925hPa(3rd row). The 1st column represents T deviation from the Raob experiment, the 2nd column the debiased (MERRA method) experiment, the 3rd column the debiased (DKM2007 method) experiment, and the 4th column the climatological bias correction method. [K]

4.5 Conclusions for Chapter 4

In this chapter, we focus on the instability of the imperfect SPEEDY-LETKF analysis system without specific humidity analysis, and applying the "climate jumps" minimization strategies to this system as done in the other stable imperfect system described in Chapter 3.

SPEEDY is a spectral model, which is advanced in comparison to the grid-point model because it is very accurate in computing space derivatives, and more computationally efficient. However, negative values in physical space may occur for some positive value variables, such as orography and humidity, known as Gibbs phenomenon. The negative humidity values are generated from SPEEDY forecast at the top 3 levels, where the real humidity is extremely low. So the specific humidity analysis is turned off at these levels in order to achieve a more stable system.

In our imperfect SPEEDY-LETKF system, the "nature run" is integration from a coupled SPEEDY-NEMO ocean model. Here, SPEEDY Version 41 is coupled to NEMO ocean model. However, the SPEEDY Version 32 that we use has climatological SST. So the climate of "nature" is different from that of the forecast model. To be more specific, we found that the "nature" climate in NH summer is hotter and more humid than the forecast model climate. The model bias evolves and accumulates nonlinearly with time, and finally makes the analysis system unstable.

We found two methods to avoid the blow-ups. One is through TRUNCT filtering and setting negative humidity values to zero. This method succeeded in removing the "Gibbs ripples" in the temperature field (Figure 4.6), but not in the surface pressure. The other method is through turning off the humidity analysis. This method can stabilize the imperfect SPEEDY-LETKF system, but leads to very biased humidity estimation and wrong physical parameterizations. So the "Gibbs ripples" still exist and the 925hPa specific humidity and temperature RMSEs grow up dramatically during the first 3 months of integration (Figures 4.7). Using these two stable SPEEDY-LETKF systems, the MERRA method, the DKM2007 method, and a climatological bias correction performed *a posteriori* are tested.

Results from the "TRUNCK" filtering plus no-negative-Q method system are shown in Chapter 3. We note that the imperfect SPEEDY-LETKF system error increase during the first 3-6 months of the analysis because we set all negative humidity outputs at the lowest 4 levels to zero and thus add a humidity source into this system. Professor Eugenia Kalnay suggested using other strategies to remove the negative humidity outputs, e.g. "borrow" the replacement of the negative humidity output at a given grid point from the nearest non-negative humidity value. It will be worth devoting further efforts to study better stabilization strategies of an imperfect SPEEDY-LETKF system.

The conclusions from the no-Q-analysis system are:

- When calculating the correction terms, we found that the "Gibbs ripples" phenomenon exists in the analysis increment difference (between RaobAirs and Raob analyses) field. The Fourier transform with 2-term truncations succeeds in representing the monthly mean of the analysis increment differences and filtering sampling noise.

- The results from the biased Raob analysis, and the three debiased analyses are compared with the RaobAirs analysis. This is because we don't know the "truth" in real life, so the best reanalysis is treated as a reference. Although blow-up is avoided, the imperfect SPEEDY-LETKF system is skewed and the correction methods through changing model tendencies do not work.

Chapter 5 Summary and future directions

5.1 Impacts of introducing new observing systems in a reanalysis

A reanalysis is performed baswed on an observing system and a meteorological forecast/data assimilation system. Even with a fixed forecast model and analysis scheme, the temporal inconsistency of the observing systems is an unavoidable issue all reanalyses need to address. Although increasing numbers and types of observing systms, especially satellite data, presents opportunities for constructing a more accurate and complete description of the global climate states, it also leads to discontinuities and spurious variations in the reanalysis. These artificial discontinuities or "jumps" in reanalyses may be caused by the assimilation of biased observations, or by introducing new observations that constrain previously unobserved components of model bias. For example, the significant changes of MERRA global mean precipitation time series in the last two decades are observed simultaneously with introducing (or ceasing) different types of satellite observations like SSMI and ATOVS. Several previous studies had explored the impacts of changing global observing system on some reanalyses like ERA40 and the creation of climatological jumps but no solution has been yet found.

5.2 Proposed solutions to minimizing reanalysis jumps due to the introduction of new observing systems

The aim for this dissertation is to find a solution, using data assimilation techniques, to minimize the "jumps" in the reanalysis long-term climate trend due to the new observing systems. The bias between an atmospheric model attractor and the real atmospheric attractor is shown in schematic Figure 3.1. For an imperfect system, the atmospheric model climate is different from the real atmospheric climate. Changes in observation systems lead to "jumps" of the model climate. However, for a perfect system, the climate of the model and that of the real atmosphere are the same. In this case, the climate depicted by the reanalysis is not impacted by changing observing systems.

The original idea of using a data assimilation technique came from Dr. Junye Chen, based on his exploration of the effects of satellite observing system changes (e.g. SSM/I in late 1987, AMSU-A in late 1998) on MERRA water and energy fluxes budgets (Chen et al. 2010, Robertson et al. 2011).

The new correction methodology is inspired by Danforth et. al (2007). In Danforth et al (2007)'s research, a 6-hourly model forecast started from a reanalysis (the NCEP-NCAR reanalysis) was compared with the verifying reanalysis to generate a bias correction forcing term, which was then added to the model tendency equation. The

model was run again for several years including the new tendency equation, and this much reduced the climatological bias.

In the present research, the analysis increment differences between a reanalysis and its corresponding Reduced Observing System Segment (ROSS) experiment are computed and, after a Fourier transform to capture the annual cycle, used as forcing terms. These forcing terms are added to the forecast model tendency. The ROSS experiment with the modified forecast model is expected to better imitate its reanalysis counterpart. This method is applied to MERRA reanalysis, whose ROSS experiment is a reanalysis using the same reanalysis system, GEOS-5 DAS, but not assimilating SSM/I observation. Humidity is the only corrected variable. The results are encouraging but only partially successful because the debiasing correction is found to be too weak. In fact, doubling the humidity correction gives results that are much closer to the original MERRA. Although the correction is just applied to humidity, other variables like precipitation, temperature, and winds also show improvements, through nonlinear model interactions generated by the moisture correction.

The reason for this underestimation, we believe, is that the analysis increments difference is not just due to the assimilation of SSMI, but to the nonlinear interactions between variables observed by AIRS and the variables that have been modified by previous assimilation of AIRS. So the correction defined by the MERRA method has

been modified by climatological bias between the forecasts of RaobAirs and Raob analyses (Equation (3.9)).

$$Correction(D\text{KM2007}) = \overline{(A_M^M - F_M^M)} - \overline{(A_M^N - F_M^M)} = \overline{(A_M^M - A_M^N)} \quad (3.8)$$

$$Correction(MERRA) = \overline{(A_M^M - F_M^M)} - \overline{(A_N^N - F_N^N)} = \overline{(A_M^M - A_N^N)} - \overline{(F_M^M - F_N^N)} \quad (3.9)$$

$$Correction(climatological) = \overline{A_M^M - A_N^N}, \; then \; \widehat{A_N^N} = A_N^N + \overline{A_M^M - A_N^N} \quad (3.10)$$

Therefore, the proper correction should be obtained by comparing the analysis increments from MERRA and from an analysis starting from MERRA at every 6-hour cycle but withholding SSMI observation in its analysis process (Equation (3.8)). This new method is named as DKM2007 method, following Danforth et al (2007)'s idea. The correction obtained using the DKM2007 method is assumed to be linear within each 6-hour analysis cycle and does not contain accumulated nonlinear errors discussed above. However, our limited computational resources prevented us from applying the DKM2007 method in the complex MERRA system.

Both of the MERRA method and the DKM2007 method are tested using a modified version of SPEEDY-LETKF system (Miyoshi 2005) provided by Dr. Ji-Sun Kang (2012), because this system is simpler, computationally inexpensive, but still realistic. The SPEEDY-LETKF analysis assimilating both RAOB and AIRS (RAOB only) is a counterpart of MERRA (NoSSMI), denoted by "RaobAirs" ("Raob"). An experiment starting from "RaobAirs" analysis but withholding AIRS observation is named "RaobAirs_noAirs".

Conducting *imperfect* SPEEDY-LETKF OSSEs is required for our purpose to improve the "climate" jumps. For this purpose, we used as nature a long integration of the coupled SPEEDY-NEMO model (courtesy of T Sluka). However, the imperfect SPEEDY-LETKF analysis is not stable and generates negative humidity values. We found two methods to stabilize the system. Following Ide and Thomas's suggestion, the first method is applying a truncation filter that eliminates spectral components outside the triangular truncation (known as TRUNCT filter) to model variables. However we also found necessary to eliminate negative humidity values in the analysis. As a result of this combined method, when assimilating RAOB only, the global RMSE of 925hPa specific humidity increases during the first 3-6 months of the analysis (Figure 3.3). The first 3 months are considered the spin-up period. Using this system, the MERRA method, the DKM2007 method, and a climatological bias correction performed *a posteriori* (Equation (3.10)) are applied. As expected, the DKM2007 method is better than the MERRA method because the corrections are not modified by the forecast differences between the RaobAirs and the Raob reanalyses. The improvement from the climatological method is not very significant because of relatively short training period.

The second stabilization strategy is not to do analysis of humidity at all. Since the humidity from this analysis is not constrained by observations, it leads to poor physical parameterizations. Although this system does not blow up, "Gibbs ripples" are still observed in its temperature field. Global RMSE of temperature at the lowest model level grows up dramatically after the spin-up period and become stabilized

after 3 month. Using this system, the "climate jumps" minimization strategies are applied, and it is shown that the MERRA approach and the DKM2007 approach do not work.

In conclusion, our goal of minimizing reanalysis "jumps" caused by new observing systems can be achieved through data assimilation techniques, or more specifically, through changing forecast model tendencies by analysis increment difference between this reanalysis and its ROSS experiment. However, if the analysis system is unstable or skewed, this correction strategy does not function. The DKM2007 method defined correction terms are not modified by the background differences between the reanalysis and its ROSS and outperforms the MERRA method.

These experiments suggest that the optimal approach to removing the reanalysis climatological jumps due to introducing (or stopping) new observing systems is the method based on the Danforth et al. (2007) approach, namely to perform a, say, two year ROSS experiment during the reanalysis with the new observing systems, and find the difference between the analysis increment with the complete observing system, and that obtained using the same 6hr forecast, but without including the new observing system. Although our OSSE results with an imperfect model are encouraging, these conclusions need to be validated using a more realistic data assimilation system with real, rather than simulated observations, e.g. the GFS-LETKF at T126 (Lien 2014)

Abbreviations and Glossary

AIRS: Alliance of Information and Referral Systems

AMSU: Advanced Microwave Sounding Unit

ATOVS: Advanced TIROS Operational Vertical Sounder

CLSM: Catchment Land Surface Model

CMAP: CPC Merged Analysis of Precipitation

CRTM: Community Radiative Transfer Model

DKM2007: a paper, Estimating and Correcting Global Weather Model Error, published by Danforth, C. M., E. Kalnay and T. Miyoshi in 2007

ERA40: 40-year ECMWF re-analysis

ESMF: Earth System Modeling Framework

GEOS-5: The Goddard Earth Observing System Model, Version 5

GPCP: Global Precipitation Climatology Project

GSI: Gridpoint Statistical Interpolation

JCSDA: Joint Center for Satellite Data Assimilation

LETKF: Local Ensemble Transform Kalman Filter

MERRA: the NASA's Modern Era Retrospective-analysis for Research and Applications

NEMO: Nucleus for European Modelling of the Ocean

OSSE: Observing System Simulation Experiment

RAOB: Universal RAwinsonde OBservation program

ROSS: Reduced Observing System Segment

SPEEDY: Simplified Parameterizations, privitivE-Equation DYnamics

SSM/I: The Special Sensor Microwave Imager

TRMM: Tropical Rainfall Measuring Mission

Bibliography

Bacmeister, J.T., M.J. Suarez, and F.R. Robertson, 2006: Rain re-evaporation, boundary-layer/convection interactions and Pacific rainfall patterns in an AGCM, J. Atmos. Sci., 8, SRef-ID: 1607- 7962/gra/EGU06-A-08925.

Baek, Seung-Jong, et al. "Correcting for surface pressure background bias in ensemble-based analyses." Monthly Weather Review 137.7 (2009): 2349-2364.

Bengtsson, L., HODGES, K. I., & HAGEMANN, S. (2004). Sensitivity of the ERA40 reanalysis to the observing system: determination of the global atmospheric circulation from reduced observations. Tellus A, 56(5), 456-471.

Bloom, S. C., et al. "Data assimilation using incremental analysis updates." Monthly Weather Review 124.6 (1996): 1256-1271.

Bosilovich, M. G., F. Robertson and J. Chen 2011. Global Energy and Water Budgets in MERRA. *J. Climate*, **24**, 5721-5739

Chen, J., M.G. Bosilovich and F. Robertson (2010, September). The Impact of ATOVS Radiance in MERRA Reanalysis. In 17th Conference on Satellite Meteorology and Oceanography.

Chen, J., and M. Bosilovich, 2012. Impacts of ATOVS and SSM/I Data in MERRA Reanalysis. *92nd Annual Meeting of the AMS*.

Cullather, Richard I., and Michael G. Bosilovich. "The moisture budget of the polar atmosphere in MERRA." Journal of Climate 24.11 (2011): 2861-2879.

Danforth, C. M., E. Kalnay and T. Miyoshi 2007. Estimating and correcting global weather model error. *Mon. Wea. Rev.***134**, 281–299

Dee, D. P., Uppala, S. M., Simmons, A. J., et al. (2011), The ERA-Interim reanalysis: configuration and performance of the data assimilation system. Q.J.R. Meteorol. Soc., 137: 553–597. doi: 10.1002/qj.828

Greybush, S.J., et al. "Balance and ensemble Kalman filter localization techniques." Monthly Weather Review 139.2 (2011): 511-522.

Hunt, B. R., E. J. Kostelich, and I. Szunyogh, 2007: Efficient data assimilation for spatiotemporal chaos: A local ensemble transform Kalman filter. Physica D, 230, 112–126, doi:10.1016/j.physd.2006.11.008.

Kalnay, Eugenia. Atmospheric modeling, data assimilation, and predictability. Cambridge university press, 2003.

Kang, J. S. (2009). Carbon cycle data assimilation using a coupled atmosphere-vegetation and the Local Ensemble Transform Kalman Filter.

Kang, J. S., Kalnay, E., Miyoshi, T., Liu, J., & Fung, I. (2012). Estimation of surface carbon fluxes with an advanced data assimilation methodology. Journal of Geophysical Research: Atmospheres (1984–2012), 117(D24).

Kennedy, A.D., X.Dong, B.Xi, X.Xie, Y.Zhang, and J.Chen, 2011. A Comparison of MERRA and NARR Reanalyses with the DOE ARM SGP Data. *J. Climate*, **24**, 4541-4557

Kim, J.-E. and M. J. Alexander 2013. Tropical Precipitation Variability and Convectively Coupled Equatorial Waves on Submonthly Time Scales in Reanalyses and TRMM, *J. Climate*, **26**, 3013-3030

Kleist, D. T., D. F. Parrish, J. C. Derber, R. Treadon, W. S. Wu, and Lord, S. 2009. Introduction of the GSI into the NCEP global data assimilation system, *Weather and Forecasting*, **24(6),** 1691-1705.

Koster, R.D., M.J. Suárez, A. Ducharne, M. Stieglitz, and P. Kumar, 2000: A catchment-based approach to modeling land surface processes in a GCM, Part 1, Model Structure. *J. Geophys. Res.*, **105**, 24809- 24822.

Krishnamurti, Tiruvalam Natarajan, ed. An introduction to global spectral modeling. Springer, 2006.

Lien, Guo-Yuan. "Ensemble assimilation of global large-scale precipitation." (2014).

Lin, Shian-Jiann. "A "vertically Lagrangian" finite-volume dynamical core for global models." Monthly Weather Review 132.10 (2004): 2293-2307.

Lindberg, Craig, and Anthony J. Broccoli. "Representation of topography in spectral climate models and its effect on simulated precipitation." Journal of climate 9.11 (1996): 2641-2659.

Lindsay, R., M. Wensnahan, A. Schweiger, and J. Zhang 2014. Evaluation of Seven Different Atmospheric Reanalysis Products in the Arctic. *Journal of Climate*, **27(7),** 2588-2606.

Lorenz, C., and J. Kunstmann 2012, The Hydrological Cycle in Three State-of-the-art Reanalyses: Intercomparison and Performance Analysis, *J. Hydrometeor*., **13**, 1397-1420

Mapes, B. E., & Bacmeister, J. T. (2012). Diagnosis of tropical biases and the MJO from patterns in the MERRA analysis tendency fields. Journal of Climate, 25(18), 6202-6214.

Miyoshi, T., 2005: Ensemble Kalman filter experiments with a primitive-equation global model, Ph.D. dissertation, University of Maryland, College Park, 197 pp.

Miyoshi, T. (2011), The Gaussian approach to adaptive covariance inflation and its implementation with the local ensemble transform Kalman filter, Mon. Weather Rev., 139, 1519–1535, doi:10.1175/2010MWR3570.1.

Molteni, 2003: Atmospheric simulations using a GCM with simplified physical parametrizations. I: model climatology and variability in multi-decadal experiments. Clim. Dyn., 20, 175–191, doi:10.1007/s00382-002-0268-2.

Pawson, Steven, et al. "Stratospheric transport using 6‐h‐averaged winds from a data assimilation system." Journal of Geophysical Research: Atmospheres (1984‐2012) 112.D23 (2007).

Reichle, R.H., R.D. Koster, G.J.M. De Lannoy, B.A. Forman, Q. Liu, S. Mahanama, and A. Toure. 2011. Assessment and Enhancement of MERRA Land Surface Hydrology Estimates. J. Climate, **24**, 6322-6338

Riddaway, R.W. and M. Hortal. "Numerical methods". March 2001 (http://old.ecmwf.int/newsevents/training/rcourse_notes/NUMERICAL_METHODS/NUMERICAL_METHODS/Numerical_methods7.html)

Rienecker, M. M., Suarez, M. J., Gelaro, R., Todling, R., Bacmeister, J., Liu, E.,& Woollen, J. (2011). MERRA: NASA's modern-era retrospective analysis for research and applications. Journal of Climate, 24(14), 3624-3648.

Robertson, F. R., Bosilovich, M. G., Chen, J., & Miller, T. L. (2011). The effect of satellite observing system changes on MERRA water and energy fluxes. *Journal of Climate*, **24(20),** 5197-5217.

Royer, Jean-Francois. "Correction of negative mixing ratios in spectral models by global horizontal borrowing." Monthly weather review 114.7 (1986): 1406-1410.

Schubert, S., and Coauthors, 2008: Assimilating earth system observations at NASA: MERRA and beyond. Extended Abstracts, Third WCRP Int. Conf. on Reanalysis, Tokyo, Japan, WCRP, **V1-103**.

Silberman, I. S. 1954, Planetary waves in the atmosphere. J. Meteorol., 11, 27-34.

Sterl, Andreas. "On the (in) homogeneity of reanalysis products." Journal of Climate 17.19 (2004): 3866-3873.

Stieglitz, M., A. Ducharne, R.D. Koster, and M.J. Suarez, 2001: The impact of detailed snow physics on the simulation of snow cover and subsurface thermodynamics at continental scales. J. Hydromet., 2, 228-242.

Suarez, M. J., Rienecker, M. M., Todling, R., Bacmeister, J., Takacs, L., Liu, H. C. & Nielsen, J. E. (2008). The GEOS-5 Data Assimilation System-Documentation of Versions 5.0. 1, 5.1. 0, and 5.2. 0.

Wang X, David Parrish, Daryl Kleist, Jeffrey Whitaker. (2013) GSI 3DVar-Based Ensemble–Variational Hybrid Data Assimilation for NCEP Global Forecast System: Single-Resolution Experiments. Monthly Weather Review **141:11**, 4098-4117.